Egypt. J. Chem. **Vol. 65,** No. SI:13B pp. 845 - 867 (2022)

Egyptian Journal of Chemistry

http://ejchem.journals.ekb.eg/

Experimental and theoretical insights into synthesized Gemini corrosion inhibitor for X65-steel in 1M HCl

Ahmed. Nasser [a*], N. M. EL Basiony [a,b], M. A. Migahed [a], H. M. Abd-El-Bary [c], Tarek A. Mohamed [c]

[a] *Egyptian Petroleum Research Institute, Nasr City 11727, Cairo, Egypt*

[b] *School of Chemical Engineering, Sungkyunkwan University, Suwon 16419, Republic of Korea*

[c] *Department of Chemistry, Faculty of Science (Men's Campus), Al-Azhar University, Nasr City 11884, Cairo, Egypt*

Abstract

Three Gemini cationic surfactants (GI-surfactants) of different hydrophobic chain lengths based on di-imine compound, abbreviated as GI-6, GI-12 and GI-14, were synthesized and characterized using FT-IR and ^{1}HNMR. The surface-active parameters calculated in acidic media were discussed. The inhibition performance of GI-surfactants for X65-steel corrosion was assessed by weight loss and electrochemical techniques in 1M HCl and was accompanied by surface analysis and theoretical studies. The resistance of X65-steel was enhanced to nearly ~764 ohm.cm^2 after adding 1x10^{-3} M of GI-14. This inferred a protective film formation on the X65-steel surface via adsorption phenomena that followed the Langmuir isotherm. The GI-surfactants' inhibition efficiency exceeded 95% at room temperature and 93 % at 328 K owing to the electron-rich centers' presence in their chemical structures. The relation between the prepared GI-surfactants molecular structures and their corrosion inhibition performance was studied theoretically based on DFT and MCs methods. The safeguard effect of GI-surfactants was confirmed by SEM and EDX. The comparison study between the GI-surfactants' performance and the previously reported compounds confirmed their high potential applications as corrosion inhibitors.

Keywords: X65-steel; Corrosion; Gemini surfactant; CMC; EIS; DFT.

1. Introduction

The natural tendency for most metals to react with moisture and oxygen causes' corrosion; in addition to that, metals like to restore their natural occurrence. The common industrial material that is widely used is carbon steel due to its unique metallic features [1]. HCl takes part in various industrial applications especially in the petroleum field in acidizing and acid cleaning processes. Generally, HCl has offensive action against metallic structures, and this led to economic loss [2]. This dilemma urged scientists to mitigate the HCl effect in industrial processes [3]. Corrosion inhibitors were classified into major groups: organic, inorganic, and a mixture of them. Surfactants "Surface-active organic compounds" could effectively use for corrosion inhibition owing to low/simplified synthetic cost, low toxicity, and high efficiency [4, 5].

Gemini surfactants which contain two hydrophilic and two hydrophobic groups and separated by a spacer were considered a subclass of cationic surfactants. Better solubility and highly efficient surface properties of Gemini surfactants with low values of both CMC and surface energy superior to those of conventional surfactants make Gemini cationic surfactants have a probable application in several scientific and industrial fields [6, 7]. The effectiveness of an inhibitor was powerfully related to its concentration, chemical structure [8]. Hegazy et al. [9] documented a detailed study on the influence of 4,4′-(((1E,5E)-pentane-1,5-diylidene)bis(azanylylidene))bis (1-dodecylpyridin-1-ium) bromide (SCGS) on steel corrosion in 1M HCl. The results revealed that SCGS form a stable complex on steel surface when adsorbed on it. Moreover, the inhibition efficiency of the metal corrosion that was elevated by increasing both the SCGS's concentration and the applied temperature values attained IE% 95.5 at 1x10^{-3}. Tawfik.M [10] discussed the influence of three ionic liquid based Gemini cationic surfactants (G2IL, G3IL and G6IL) on carbon steel in 1M HCl, where he found that the prepared compounds could inhibit corrosion on the carbon steel surface by adsorbing on it, in which the inhibition efficiency increases with increasing their concentration but decreases with increasing temperature. Recently, the study of the inhibition action of Gemini surfactants in several aggressive media got a lot of attention [11, 12]. Gemini cationic surfactant had enhanced adsorption ability on metal surfaces that shields surface from the

*Corresponding author e-mail: **Ahmed. Nasser**, ahmednasser1992@outlook.com

Receive Date: 24 July 2022, Revise Date: 15 August 2022, Accept Date: 18 August 2022

DOI: 10.21608/EJCHEM.2022.152233.6594

destructive media owing to the existence of centers with high electron density such as (N, P, π electrons, and aromatic ring) in addition to the hydrophobic chain [13].

Therefore, we have initiated the current study on three Gemini surfactants (GI-surfactants) that contain quaternarization centers with long aliphatic chain to facilitate their adsorption on the surface of X65-steel and then improve their corrosion inhibition efficiency. The efficiency of the new synthesized surfactants is higher than the other organic inhibitors because of surfactant compounds exist at the interface between corrosive media and steel surface by more concentration. Accordingly, the surfactant compounds are more efficient than the same organic compounds at the same concentration. To the best of our knowledge, the above-mentioned synthesized surfactants have neither electrochemically nor theoretically studied for metals corrosion inhibitors in 1M hydrochloric acid.

The main target of this work is to prepare cheap, environmentally friendly, non-toxic natural compounds that could be used for acid pickling of carbon steel in acid medium. Therefore, the newly synthesized GI-surfactants have been evaluated as X65-steel corrosion in 1 M hydrochloric acid via different chemical and electrochemical techniques respectively. Also, the effect of GI-surfactants at different concentrations and temperatures on its inhibition behavior has been also studied. The correlation between GI-surfactants chemical structures and their inhibition performance studied with the aid of quantum indices parameters based on density function theory (DFT) and Monte Carlo simulation (MCs).

Finally, surface morphology and the chemical composition of outer layer of X65-steel with the aid of (SEM) and (EDX) have been studied.

2. Experimental

2.1 Chemicals

The chemicals were purchased and used in the absence of further purification with high purity grade as follow; 4-(Dimethyl amino) benzaldehyde, 1,4-Diaminobutane, and HCl (37%) of analytical grade were purchased from Alpha Chemistry Company. Ethanol and diethyl ether were purchased from Bio. Chem, Egypt. Whereas, 1-Bromohexane, 1-Bromododecane, and 1-Bromotetradecane were purchased from Aldrich, Germany.

2.2. The chemical synthesis

The inhibitors used in this work were prepared through two steps.

In the first step, the Schiff base compound ((N1Z, N4E)-N1, N4-bis (4 (dimethylamino) benzylidene) butane 1,4-diamine) was synthesized by a condensation reaction between 4-(Dimethylamino) benzaldehyde and 1,4-Diaminobutane in molar ratio 2:1 in 25 mL ethanol (EtOH), with three droplets of HCl for 7h. In the second step, three GI-surfactants were obtained by quaternization reaction of the previously prepared Schiff base separately with alkyl halides of dissimilar alkyl chain lengths (hexane-, dodecane- and tetradecane-bromide) using 1:2 molar ratio in 50 ml ethanol at 373 ±1K for 36 h [14]. The reaction mixtures were permitted to settle down, and the yields were filtered out and then rinsed with diethyl ether followed by recrystallization using ethanol to produce: 4,4'-((1Z,1'E) - (butane-1,4 diyl bis (azanylylidene)) bis (methanylylidene)) bis (N- hexyl-N,N - dimethyl benzeneaminium) bromide (**GI-6**), 4,4'-((1Z,1'E) - (butane-1,4 diyl bis (azanylylidene)) bis (methanylylidene)) bis (N- dodecyl- N,N - dimethyl benzeneaminium) bromide (**GI-12**) and 4,4'-((1Z,1'E)-(butane-1,4- diyl bis (azanylylidene)) bis (methanylylidene)) bis (N, N- dimethyl-N- tetradecyl benzenaminium) bromide (**GI-14**), respectively, as shown in Scheme 1. The final products were filtrated and dried to attain the prepared GI-surfactants.

The synthesized GI-surfactants' chemical structure was distinguish using FT-IR and ^{1}HNMR spectral analysis. The IR spectra of the powdered sample were verified on Shimadzu FTIR-8300. While the ^{1}HNMR spectra were verified on Bruker Spectro spin instrument at 500 MHz Ultra Shield magnets [15] with the sample dissolved in DMSO-d_6.

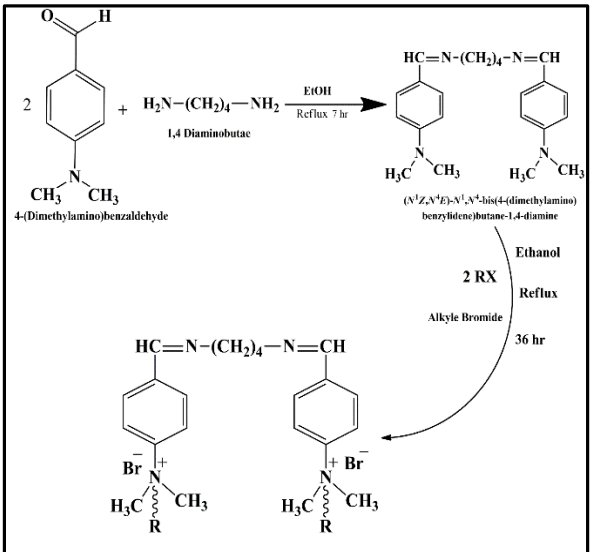

Scheme 1 Syneses of Chemical structure of the prepared gemini surfactants

2.3. Steel specimen

Iron (Fe) was the major component in the chemical analysis of X65-steel and the residue was: 0.210 % Si, 0.103 % C, 0.024 % P, 0.012 % Ni, 1.05 % Mn, and 0.032 % Co.

2.4. Surface tension calculations

Surface tension of the freshly synthesized (GI-6, GI-12, and GI-14) surfactants solutions at 298 ±1K were calculated by using Tensiometer-K6 processor (Krüss Company, Germany) by using Pt ring method [16]. For each experiment surface tension of 1M, HCl was obtained and among the measurement runs, the ring was cleaned with acetone followed by deionized water.

2.5. Solutions

1M of hydrochloric acid is freshly prepared, used as a corrosive medium and $1x10^{-2}$ M stock solution of three GI-surfactants in 1 M HCl were prepared followed by acid dilutions to obtain concentration range from $1x10^{-5}$ to $1x10^{-3}$ M of the investigated GI-surfactants at 298 ±1K.

2.6. Weight loss measurements

This method is easy and reliable to assess the corrosion rate and inhibition effect of an inhibitor [17]. A clean weighed of X65-steel sheets with dimensions (4.7 × 1.8 × 0.14) cm is fully immersed for 6*h* in a bottle 0.1 L of 1M HCl without and containing series concentrations ($1x10^{-5}$ to $1x10^{-3}$ M) of the prepared GI-surfactants at 298 ±1K. The effect of high temperature on the performance of the prepared surfactant in range (298-328 ±1K) can be understood using weight loss measurement in the existence of $1x10^{-3}$ M of GI-surfactants in 1M HCl solution.

2.7. Electrochemical measurements

Electrochemical procedures were accomplished by using Auto-lab (PGSTAT-128N) potentiostat/ galvanostat in an ordinary electrolytic jacketed glass cell, 0.1 L, through a three-electrode system as follow: platinum sheet as auxiliary electrode, X65-steel as a working electrode and Ag/AgCl/(3M KCl) as reference electrode (connected to electrochemical system via luggin capillary tube). All measurements were managed at 298 ±1K. X65-steel electrode was cut into cylindrical shape and shielded with epoxy resin leaving a surface area of $1cm^2$ to contact the solution. Before running all experiments, X65-steel surface area was abraded with emery paper of dissimilar grades from 600 to 2500, cleaned twice with distilled water and acetone. X65-steel electrode was engrossed for 30 min. in a test solution until a steady state (*E*ocp) was attained.

Electrochemical impedance spectroscopy (EIS) was executed at E_{opc} in a frequency range of 100000-0.1 HZ with an amplitude of 10 mV peak to peak using AC signals. For the inhibition efficiency calculations (IE %), charge transfer resistance (R_{ct}) values were used as a function in IE% values of EIS according to the following equation [18]:

$$IE\% = (1 - R_{ct(blank)}/R_{ct(inh)}) \times 100 \quad (1)$$

where, $R_{ct(blank)}$ and $R_{ct(inh)}$ are the X65-steel charge transfer resistances free and with GI-surfactants, respectively. Potentiodynamic polarization (PDP) measurements were used to determine the cathodic and anodic polarization curves of X65-steel in blank HCl, and after treatment with dissimilar concentrations of GI-surfactants. PDP curves were attained by varying the electrode potential in range of ± 400 mV around the open circuit potential at a scan rate of 1 mV/S. The IE% values were intended according to the next equation [19]:

$$IE\% = (1 - i_{corr}/i^{\circ}_{corr}) \times 100 \quad (2)$$

where, i_{corr} and i°_{corr} represent the values of specific corrosion current density with and free GI-surfactants molecules, respectively. Nevertheless, Nova 2.1.4 software has been used to fit the electrochemical data. All the measured potentials were referred to the Ag/AgCl electrode potential.

2.8. SEM/EDX study

The surface analysis study of X65-steel surface immersed in HCl for 6*h* has been executed with the aid of Scanning electronic microscope (SEM) [20, 21], linked with Energy Dispersive X-ray spectroscopy (EDX) unit before and after addition ($1x10^{-3}$ M) of GI-14 surfactant at 298 ±1K. QUANTA FEG-250 (Field Emission Gun) instrument model is selected to perform the X-65-steel surface analysis.

2.9. Computational studies

Geometry optimization and quantum chemical calculations for the three GI-surfactants were obtained in a vacuum and solvated phases with convergence tolerance of medium quality using VAMP module. Based on density functional theory (DFT) [22], the chemical parameters were attained from the Hamiltonian neglect of diatomic differential overlap (NDDO) with the parameterized element modified neglect of differential overlap (MNDO) using BIOVIA Materials Studio 17.1.0.48 software. The calculated parameters embrace the energy of highest occupied molecular orbital (E_{HOMO}, eV), energy of lowest unoccupied molecular orbital (E_{LUMO}, eV), energy gap (ΔE, eV = E_{LUMO}− E_{HOMO}), electron affinity (*A*), ionization potential (*I*), electronegativity (χ), softness (σ), hardness (η) and number of the electron transferred (ΔN) [23].

The adsorption energies of the three GI-surfactants on X65-steel surface were intended from Monte Carlo simulation (MCs) supported by the adsorption locator module in Material Studio software. The MCs has been operated in vacuum and solvent phases. The

adsorption energy ($E_{ads.}$) attained from the interaction between GI-surfactants and the X65-steel surface was intended by introducing the greatest stable Fe crystal with surface cleavage (1 1 0). MCs process was performed in a simulated box with the following dimensions in Angstroms (49.6 x 49.6 x 24.05) with periodic boundary conditions and the cleavage plane was expanded to a (20 ×20) supercell. And then 15 Å vacuum slab was built over Fe (1 1 0) plane to eliminate the periodic boundary effect. The annealing simulated process of (MCs) was done through 10 cycles with 15000 steps individually till reaching optimization for surfactant/ Fe (1 1 0) system, where the total energy of the system fluctuated about the mean value. The force field was set to COMPASS with medium quality of the energy calculation.

3. Results and discussion

3.1. Structure confirmation

The chemical structure of the prepared GI-surfactants in Scheme 1 was confirmed by FTIR and ^{1}HNMR spectra. Primary, the FTIR spectrum displayed the principal characteristic bands of the synthesized surfactant (GI-14) as a representative one in Fig. 1. IR (υ, cm^{-1}): 2926.75 (**C-H** asymmetric), 2812.07 (**C-H** symmetric), 1605.63 (**C=N**), 1445.41 (**C=C** aromatic), 813.32 (**C-H** $_{\text{alkene bend}}$). ^{1}HNMR (DMSO-d$_6$, ppm) spectrum of the synthesized surfactant (GI-14) was exposed in Fig. 2. The spectrum displayed different bands at: δ 3.35(s, 12 H, 4 CH_3), 1.59 (m, 4H, 2CH_2), 3.47 (t, 4H, 2CH_2), 6.8 (d, 2H, J = 8.11 Hz, Ar-H), 7.6 (d, 2H, J = 8.21 Hz, Ar-H), 8.12 (s, 2H, CH $_{\text{enaminic}}$), 2.9(t, 4H, 2CH_2), 1.68 (m, 4H, 2CH_2), 1.22 (m, 44H, CH $_{\text{aliphatic chain}}$), 0.88 (d, 6H, 2$CH_3$).

3.2. Surface active properties

3.2.1. Critical micelle concentration (C_{cmc}) and Surface tension (γ_{cmc})

Surface active properties of GI-surfactants were measured at 298 ±1K, an increase of adsorbed surfactant molecules with their gradually increased concentration at HCl/air interface caused a decreasing in the surface tension. The C_{cmc} values of GI-surfactants were calculated from the intersection between (γ) and ($-\log C$) (Fig. 3 and Table 1) [24]. The C_{cmc} was directly proportional to the number of methylene moieties (hydrophobic chain length) in the order: GI-14 > GI-12 > GI-6. The result ensured an inversely proportional correlation between surface tension and the molar concentration of the GI-surfactants until reaching the CMC. After the critical concentration, almost a steady surface tension was obtained (Fig. 3). Consistent outcomes were revealed from Table 1, where γ_{cmc} of GI-14 was the smallest value, hence the more densely (bulky) the GI-surfactants the more adsorption occurs at air/HCl interface [25].

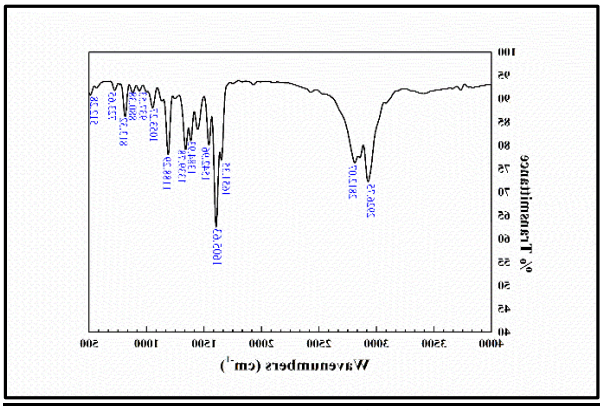

Fig 1: FTIR spectrum of GI-14

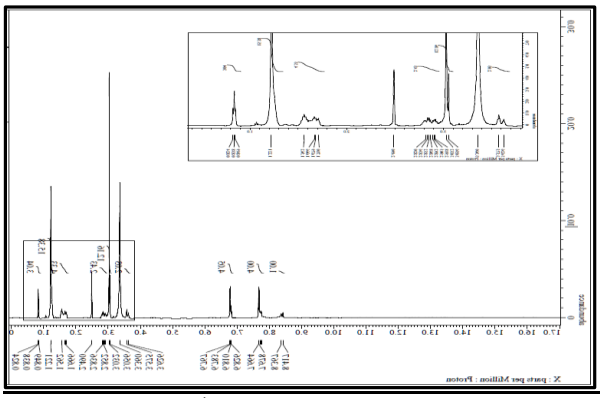

Fig 2: ^{1}H NMR spectrum of GI-14

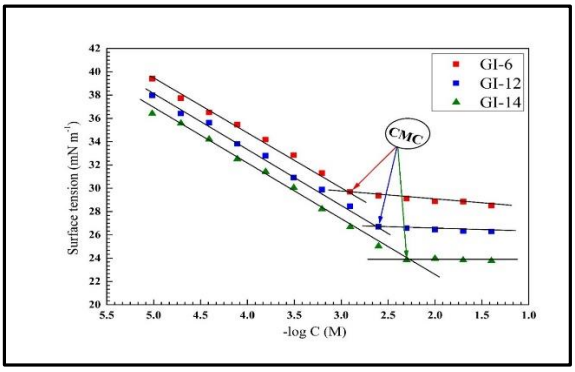

Fig 3: Variation of the surface tension with the prepared GI-surfactants concentrations in water at 298 ±1K.

Table (1): Surface properties of the synthesized GI-surfactants in 1 M HCl at 298 ±1K.

Inh.	*CMC (^{3}-mol dm)*	*γ_{cmc} (mN m^{-1})*	*π_{cmc} (mN m^{-1})*	*$\Gamma_{max.}$ (mol cm^{-2})*	*$A_{min.}$ (nm^2) x10^{-7}*
GI-6	*0.00125*	*29.6*	*30.4*	*0.00019*	*8.339*
GI-12	*0.0025*	*26.5*	*33.5*	*0.00023*	*7.101*
GI-14	*0.005*	*23.5*	*36.5*	*0.00027*	*6.055*

3.2.2. Effectiveness (π_{cmc})

The above-calculated surface tension values γ_{cmc} was correlated to the effectiveness (surface

pressure; π_{cmc}) for the GI-surfactants (Table 1) using the equation [26]:

$$\pi_{cmc} = \gamma_{o} - \gamma_{cmc} \quad (3)$$

where γ_{o} and γ_{cmc} were the surface tension of HCl (60 mN/m) at the assigned temperature and the surface tension at CMC respectively. The greatest powerful inhibitor was one that gave the bigger dropping in surface tension with high efficacy value at CMC where the GI-14 (π_{cmc}= 36.5 mN/m) was the greatest effective one with the lowest surface tension compared to 33.5 and 30.4 (π_{cmc}) for GI-12 and GI-6 surfactant, respectively [27].

3.2.3. Maximum Surface Excess (Γ_{max})

Γ_{max} of GI-surfactants solution is the quantity of GI-surfactants molecules per unit area at the solution/air interface, it was intended from the slope (d γ/dlnC) of a linear plotting of (γ) against (lnC) according to Gibbs's adsorption equation [28]:

$$\Gamma_{max} = (-1/nRT)(d\gamma/dlnC) \quad (4)$$

where C was the concentration of the prepared GI-surfactants, R was the universal gas constant, T was the absolute temperature and γ represented the surface tension. The n value was taken as 3 for a dimeric compound made up of divalent ion and two univalent counter ion in the absence of a swamping electrolyte [29]. Similar to the above-mentioned results, Γ_{max} was directly proportional to number of methylene moieties, i.e., bulky GI-surfactants were firmly packed in the solution/air interface (Table 1). Note that GI-14 surfactant had high maximum surface excess (Γ_{max}= 0.00027) compared with the GI-12 and GI-6 surfactants (Γ_{max}= 0.00023 and 0.00019), respectively.

3.2.4. Minimum surface area (A_{min})

Quantitatively in nm^2 at the solution/air interface, the degree of packing and the orientation for each adsorbed inhibitor molecule could be effectively described with the aid of minimum surface area (A_{min}). A_{min} was function in Γ_{max} according to the following equation [30]:

$$A_{min} = 10^{14}/(N_A\, \Gamma_{max}) \quad (5)$$

where, N_A was the Avogadro's number and Γ_{max} was the maximum surface excess as per listed in Table 1. Larger values of Γ_{max} designated a higher number of adsorbed molecules at solution/air interface. Hence, the available area for each molecule was reduced at the surface interface. According to data attained in Table 1 it was obvious that, increasing the alkyl chain length led to a decreasing in A_{min}: the area occupied by each molecule. The discussed surface-active parameters indicated the affinity of GI-surfactants molecules to be adsorbed at the interface therefore, the studied GI-14 surfactant had a higher tendency to cover/protect the X65-steel surface against the corrosive media than GI-12 and GI-6, enhanced surface shield against corrosion.

3.3. Weight loss measurements

3.3.1. Effect of concentration

At room temperature (298 ±1 K), average weight loss (ΔW) could be obtained by subtracting the initial (W_o) and final (W) weights of the X65-steel coupons after immersion for 6*h* in corrosion test media. Moreover, the rate of corrosion *CR* (mg cm^{-2} h^{-1}), surface coverage (θ), and the inhibition efficiency (IE %) of the prepared surfactants could be calculated using the following formulas [31]:

$$CR = \frac{\Delta W}{S\,d\,t} \quad (6)$$

$$\theta = \left(\frac{\Delta W - \Delta W}{\Delta W_o}\right) \quad (7)$$

$$IE\,\% = \theta x 100 \quad (8)$$

where S, was the surface area of the X65-steel specimen (cm^2), t, was the immersion time (6*h*), and d, was iron density (7.85 g.cm^{-3}). The *CR*, IE %, and θ were attained from ΔW of X65-steel coupons in 1M HCl before and after immersion with the GI-surfactants "inhibitors" at the selected concentration range (1*x*10^{-5} to 1*x*10^{-3} M) (Table 2). In agreement with Ref. [32], the corrosion rate simultaneously decreases by increasing the concentration of surfactants. High inhibition efficiency was observed at 1*x*10^{-3} M of the GI-surfactants; 95%, 96%, and 97% for GI-6, GI-12, and GI-14, respectively. This significantly increased the strength of the adsorption film formed on the iron surface coupons via the high electron density centres exist on surfactant molecules side by side to the alkyl chain length which the intensity of adsorbed protective film over X65-steel surface. The GI-surfactants' efficacy increased by increasing chain length (from 6 to 14). This behavior is due to the fact that the adsorption coverage of inhibitor on X65-steel surface increases with the inhibitor concentration. Note that, the bulky methylene alkyl chain kept the aggressive Cl$^-$ anions away from X65-steel surface [33], which led to high protection and highest inhibition efficiency in case of GI-14 surfactant.

Table (2): Corrosion parameters obtained from weight loss measurements of X65-steel coupons after 6*h* immersions in 1 M HCl solution with and without addition of various concentrations of the synthesized GI-surfactants at 298 ±1K.

At the optimum concentration (1*x*10^{-3} M), potential application of GI-surfactants as corrosion inhibitor for X65-steel in 1 M hydrochloric acid media could be obtained from the perseverance resistance of the film formed during exposure to harsh conditions of temperature and aggressive acid concentration:

❖ *Effect of temperature*

Generally, the iron dissolution rate increased with temperature, due to increasing the kinetic motion of electrolyte (HCl) and hydrogen gas bubbles evolved which led to desorption of the formed layer over X65-steel surface and increased the exposed area of metal subjected to HCl solution. But the dissolution rate became much lower by adding GI-surfactants related to the blank counterpart. The inhibition efficiency values of GI-surfactants at ($1x10^{-3}$ M) for the X65-steel corrosion in 1 M HCl at temperature range (298-328 ±1K) were tabulated in Table 3 and observed in Fig. 4. We can conclude from the data obtained that, higher adsorption features of GI-surfactants molecules even in high-temperature conditions were 3% loss of inhibition efficiency of GI-14 over the wide temperature rang studied. It was worth mentioning that, the inhibition efficiency was kept above 93% for all GI-surfactants implemented herein ($1x10^{-3}$ M) at severe temperature up to 328 K as might be the case in Gulf region in the summer, such efficiencies were considered good enough for corrosion inhibitor candidates. The IE% was inversely proportional to temperature which was initially devoted to a sort of an equilibrium in adsorption-desorption process of GI-surfactants, which was then shifted towards a desorption process [34]

❖ *HCl concentration*

We have carried similar investigation of the GI-surfactants at higher concentration of HCl from (2-5 M), these results were tabulated in Table 4. GI-surfactants at ($1x10^{-3}$ M) saved the corrosion inhibition resistance of X65-steel at 96.91%, 95.85%, 95.03% and 94.79% in (2, 3, 4 and 5 M HCl) respectively,

Table 4. This observed high application potential of GI-surfactants as X65-steel corrosion in acidic applications (acidizing and acid cleaning process).

Inh.	*C (M)*	*CR (g cm^{-2} h^{-1})*	*θ*	*IE (%)*
GI-6	***Blank***	*0.007*	-	-
	1x10^{-5}	*0.003*	*0.556*	***55.6***
	5x10^{-5}	*0.001*	*0.779*	***77.9***
	1x10^{-4}	*0.0007*	*0.890*	***89.0***
	5x10^{-4}	*0.0004*	*0.937*	***93.7***
	1x10^{-3}	*0.0003*	*0.952*	***95.2***
GI-12	***1x10^{-5}***	*0.0028*	*0.598*	***59.8***
	5x10^{-5}	*0.0011*	*0.842*	***84.2***
	1x10^{-4}	*0.0006*	*0.916*	***91.6***
	5x10^{-4}	*0.0004*	*0.947*	***94.7***
	1x10^{-3}	*0.0002*	*0.966*	***96.6***
GI-14	***1x10^{-5}***	*0.002*	*0.624*	***62.4***
	5x10^{-5}	*0.0009*	*0.858*	***85.8***
	1x10^{-4}	*0.0004*	*0.929*	***92.9***
	5x10^{-4}	*0.0003*	*0.951*	***95.1***
	1x10^{-3}	*0.0001*	*0.972*	***97.2***

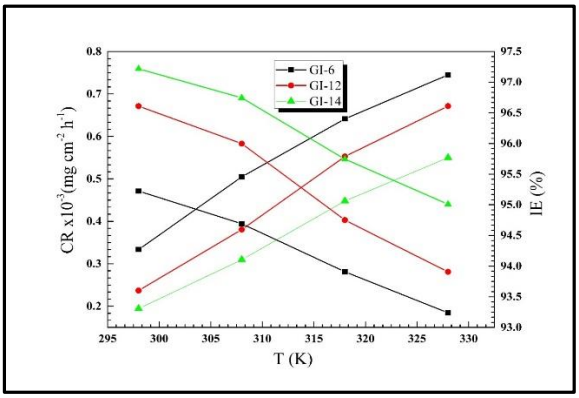

Fig 4: Influence of the temperature range (298-328) ±1K on the rate of corrosion and the inhibition performance of the prepared GI-surfactants (GI-6, GI-12, GI-14) at $1x10^{-3}$ M.

Table (3): Corrosion parameters obtained from weight loss measurements of X65-steel coupons after 6*h* immersions in 1 M HCl solution with and without addition of $1x10^{-3}$ M concentration of the synthesized GI-surfactants at different temperatures.

Inh.	*C (M)*	*Temperature*											
		***298* ±1K**			***308* ±1K**			***318* ±1K**			***328* ±1K**		
		CR (g cm^{-2} h^{-1})	***θ***	***IE (%)***	***CR (g cm^{-2} h^{-1})***	***θ***	***IE (%)***	***CR (g cm^{-2} h^{-1})***	***θ***	***IE (%)***	***CR (g cm^{-2} h^{-1})***	***θ***	***IE (%)***
GI-6	***Blank***	*0.007*	-	-	*0.0095*	-	-	*0.0105*	-	-	*0.011*	-	-
	1x10^{-3}	*0.0003*	*0.952*	*95.2*	*0.0005*	*0.946*	*94.6*	*0.0006*	*0.939*	*93.9*	*0.0007*	*0.932*	***93.24***
GI-12	***Blank***	*0.007*	-	-	*0.0095*	-	-	*0.0105*	-	-	*0.011*	-	-
	1x10^{-3}	*0.0002*	*0.966*	*96.6*	*0.0004*	*0.96*	*96*	*0.0006*	*0.947*	*94.7*	*0.0007*	*0.939*	***93.9***
GI-14	***Blank***	*0.007*	-	-	*0.0095*	-	-	*0.0105*	-	-	*0.0110*	-	-
	1x10^{-3}	*0.0001*	*0.972*	*97.2*	*0.0003*	*0.967*	*96.7*	*0.0004*	*0.957*	*95.7*	*0.0005*	*0.95*	***95***

3.4. Adsorption isotherm

Dissimilar adsorption isotherm models, Langmuir, Temkin, Frumkin, AL-Awady, Flory–Huggins and Freundlich [35] have been applied to explain the behavior of a particular inhibitor on the steel surface whether its chemical and/or physical adsorption based on weight loss data. The current GI-surfactants adsorption model on X65-steel surface followed Langmuir isotherm according to the following equation:

$$C_{\text{inh}}/_{\theta} = 1/K_{\text{ads}} + C_{\text{inh}} \qquad (9)$$

where (C_{inh}) was the inhibitor molar concentration of GI-surfactants and (K_{ads}) was the adsorption equilibrium constant. For the prepared surfactants; GI-6, GI-12, and GI-14, the Langmuir plots ($^{C_{inh}}/_{\theta}$ vs. C_{inh}) showed a straight line with good regression coefficient (R^2; 0.9999) and slope values closed to unity. The output Langmuir adsorption isotherm parameters were tabulated in Table 5, whereas the reported K_{ads} were intended from the reciprocal of the intercept of $^{C_{inh}}/_{\theta}$ vs. C_{inh} curve, Fig. 5. A large value of K_{ads} attribute to the stronger and more stable adsorbed layer formed on the metal surface favoring the investigated GI-surfactants as efficient corrosion inhibitors with a bit preference of GI-14. It has been already established that, K_{ads} was correlated to the standard free energy of adsorption (ΔG°_{ads}) inferred from the following equation [36]:

$$\Delta G^{\circ}_{ads} = -RT \ln(55.5 K_{ads}) \quad (10)$$

where T was the absolute temperature (298 K), R was the gas constant (8.314 J/mol. K) and the value 55.5 was the water molar concentration. The calculated ΔG°_{ads} of the prepared GI-surfactants at 298 K were given in Table 5. The negative value of ΔG°_{ads} assumed spontaneous/stable adsorption of GI-surfactants on the X65-steel surface. Moreover, many studies have differentiated between chemisorption and physisorption processes according to ΔG°_{ads} values. As a basic rule, ΔG°_{ads} values of -20 or lower were related to an electrostatic interaction among charged molecules and charged steel surface (physisorption), whereas values of -40 or higher were related to charge transfer between the surfactant molecules and the steel surface to procedure a coordinate covalent bond (chemisorption).

In the current study, the values of ΔG°_{ads} were -38.5, -39.1, and -39.3 (kJ mol^{-1}) for GI-6, GI-12, and GI-14, respectively.

Referring to the detailed numerical values of ΔG°_{ads} given in [37]. The adsorption of GI-surfactants on X65-steel surface is neither typical physisorption nor typical chemisorption but is a complex mixed type of chemical/physical adsorption [38], in addition, it was preferably chemical adsorption because ΔG°_{ads} values were higher and close to -40 kJ mol^{-1}.

Table (5): Standard thermodynamic parameters of the adsorption on the X56-steel surface in 1 M HCl solution containing different concentrations of the synthesized GI-surfactants at 298 ±1K.

Inh.	R^2	*Slope*	K_{ads} (M^{-1})	ΔG^{o}_{ads} (kJ mol^{-1})
GI-6	*1*	*1.04*	*103.003*	*-38.54*
GI-12	*0.9999*	*1.02*	*128.706*	*-39.10*
GI-14	*0.9999*	*1.02*	*140.121*	*-39.31*

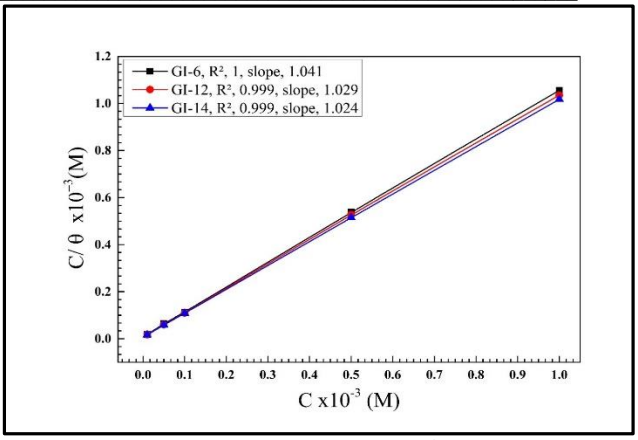

Fig 5: The Langmuir isotherm adsorption plots for X65-steel in (1.00) M HCl containing different concentrations of the synthesized GI-surfactants (GI-6, GI-12, GI-14) at 298 ±1K.

3.5. Activation thermodynamic parameters

We have also studied the thermodynamic indices (E_a; activation energy, ΔH^*; enthalpy of activation, and ΔS^*; entropy of activation) of X65-steel reaction free and with $1x10^{-3}$ M of studied GI-surfactants using Arrhenius and transition state equations [39]:

$$\ln CR = \ln K - (^{E_a}/_{RT}) \quad (11)$$

$$\ln {}^{CR}/_{T} = {}^{-\Delta H^*}/_{RT} + \ln {}^{R}/_{Nh} + {}^{\Delta S^*}/_{R} \quad (12)$$

where, *CR*, *K*, *R*, *h*, and *N* were the corrosion rate derived from the weight loss of X65-steel, Arrhenius constant, universal gas constant, Plank's constant, and Avogadro's number, respectively. Slope of ln CR Vs T^{-1} in Fig. 6 gave the value of E_a (E_a= (slope*R)), which was found higher in case of GI-surfactants than that in case of pure HCl solution, revealing the adsorption of GI-surfactants on the X65-steel surface, shielding it from the aggressive HCl medium, Table 6, [40].

The plot of ln (CR /T) against 1/T yield a linear relationship, where ($^{-\Delta H^*}/_{R}$) was the slope and ($^{\ln R}/_{Nh} + {}^{\Delta S^*}/_{R}$) was the intercept, (Fig. 7 and Table 6). The positive sign of ΔH^* indicated an endothermic nature of inhibitor adsorption on X65-steel, ΔH^* was found to be increased with the hydrophobic chain length of GI-surfactants declaring more difficult dissolution of X65-steel compared to the blank aqueous HCl [41].

Moreover, the negative sign of ΔS^* in the treated and untreated solutions indicated that decrease in disordering takes place ongoing from reactants to products activated complex [42]. This revealed that the randomness decreased as a result of adsorption of GI-surfactants on X65-steel surface. This performance can be clarified as a result of shifting water molecules and chloride ions away from X65-steel surface accompanied by the adsorption of GI-surfactants. These outcomes were well evidenced quantitatively by the ongoing EDX given below (Section 3.8) and also consistent to those revealed earlier [43, 44].

Table (4): Corrosion parameters obtained from weight loss measurements of X65-steel after 6h immersions in different concentration of HCl solution with and without addition of $1x10^{-3}$ M concentration of the prepared GI-surfactants

Inh.	C (M)	Conc. Of HCl											
		2 M			3M			4M			5M		
		CR (g cm^{-2} h^{-1})	Θ	IE (%)	CR (g cm^{-2} h^{-1})	Θ	IE (%)	CR (g cm^{-2} h^{-1})	Θ	IE (%)	CR (g cm^{-2} h^{-1})	Θ	IE (%)
GI-6	Blank	0.0154	-	-	0.0168	-	-	0.0168	-	-	0.0180	-	-
	1x10^{-3}	0.0007	0.9507	95.07	0.0008	0.9496	94.96	0.00104	0.9382	93.82	0.0013	0.9234	**92.34**
GI-12	Blank	0.0154	-	-	0.0168	-	-	0.0168	-	-	0.0180	-	-
	1x10^{-3}	0.0006	0.9608	96.08	0.0007	0.9547	95.47	0.00086	0.9492	94.92	0.0010	0.9398	**93.98**
GI-14	Blank	0.0154	-	-	0.0168	-	-	0.0168	-	-	0.0180	-	-
	1x10^{-3}	0.0004	0.9691	96.91	0.0006	0.958	95.85	0.00083	0.9503	95.03	0.0009	0.9479	**94.79**

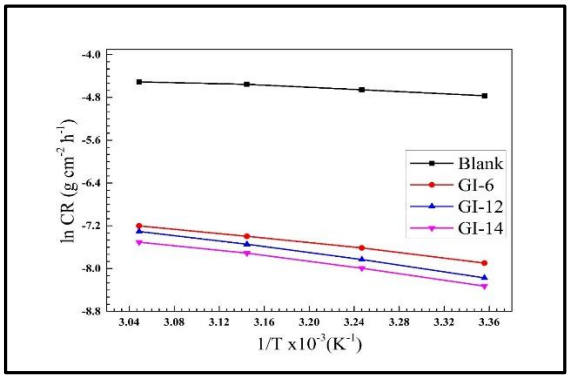

Fig 6: Arrhenius plots, variation of ln CR against 1/T, for X65-steel in (1.00) M HCl devoid of and containing $1x10^{-3}$ M of GI-surfactants.

Table (6): Activation thermodynamic parameters for X65-steel corrosion in 1 M HCl in the absence and presence of $1x10^{-3}$M of the prepared GI-surfactants.

Solution	E_a (kJ mol^{-1})	ΔH^* (kJ mol^{-1})	ΔS^* (kJ mol^{-1} K^{-1})
Blank	12.0777	9.48018	-253.793
GI-6	21.667	19.069	-246.955
GI-12	28.565	25.967	-226.714
GI-14	28.49	25.892	-228.644

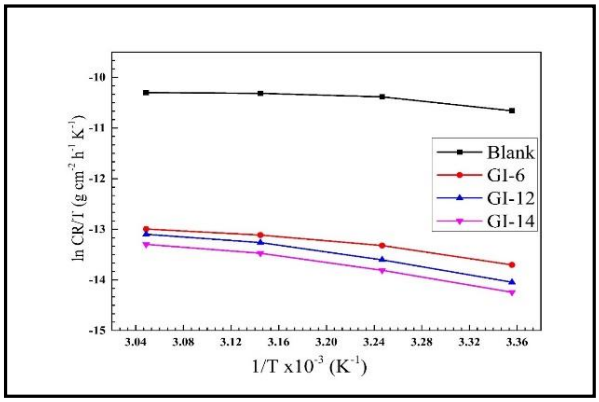

Fig 7: Transition state relation of ln (CR/T) against 1/T, for X65-steel in (1.00) M HCl devoid of and containing $1x10^{-3}$ M of GI-surfactants.

3.6. Electrochemical impedance spectroscopic study (EIS)

In the absence and presence of various concentrations of the prepared GI-surfactants (GI-6, GI-12, and GI-14) after 30 min. immersion at room temperature, the corrosion performance of X65-steel in 1 M HCl solution could be obtained with the aid of non-destructive EIS technique. EIS spectra appeared as Nyquist and bode plots as in Fig. 8 and Fig. 9 respectively. Inspection of Fig. 8 and Fig. 9, the following discussion can be obtained:

I. In high frequency (HF) region, a single capacitive loop could be obtained from the Nyquist plots with one time constant as in bode-phase plot, which indicated that a charge transfer process controlled the X65-steel redox reaction [45].

II. Also, at the center of abscissa, a depressed semicircle appeared from The Nyquist plots. Besides, in bode-phase angle plot at the intermediate frequency region, the line slopes and the phase angle values were deviated from -1 and -90° respectively see Table 7. All of those were returned to the frequency dispersal, inhomogeneities, and scabrous of the metal surface [46].

III. The shape of semicircle loops in Nyquist plots free and with dissimilar concentrations of GI-surfactants were the same without significant change, indicated that the corrosion mechanism did not change even after adding the prepared surfactants. Just the diameter of semicircle loops increased with the addition of GI-surfactants even at low concentration ($1x10^{-5}$ M) due to their effective adsorption [47].

Table (7): Slope and phase angle degree values obtained from EIS measurements for X65-steel in 1 M HCl solution in the absence and presence of different concentrations of the prepared GI-surfactants at 298 ±1K.

Inh.	*Conc. (M)*	*-Slope*	*-Phase angle°*
GI-6	***Blank***	*0.4779*	*51*
	1x10^{-5}	*0.6167*	*53*
	5x10^{-5}	*0.6994*	*60*
	1x10^{-4}	*0.7060*	*61.3*
	5x10^{-4}	*0.7499*	*64*
	1x10^{-3}	*0.7547*	*65*
GI-12	***1x10^{-5}***	*0.6220*	*55*
	5x10^{-5}	*0.6995*	*62*
	1x10^{-4}	*0.73*	*64*
	5x10^{-4}	*0.7497*	*67*
	1x10^{-3}	*0.7718*	*69*
GI-14	***1x10^{-5}***	*0.6185*	*60*
	5x10^{-5}	*0.7356*	*63*
	1x10^{-4}	*0.7530*	*67*
	5x10^{-4}	*0.8015*	*69*
	1x10^{-3}	*0.8074*	*70*

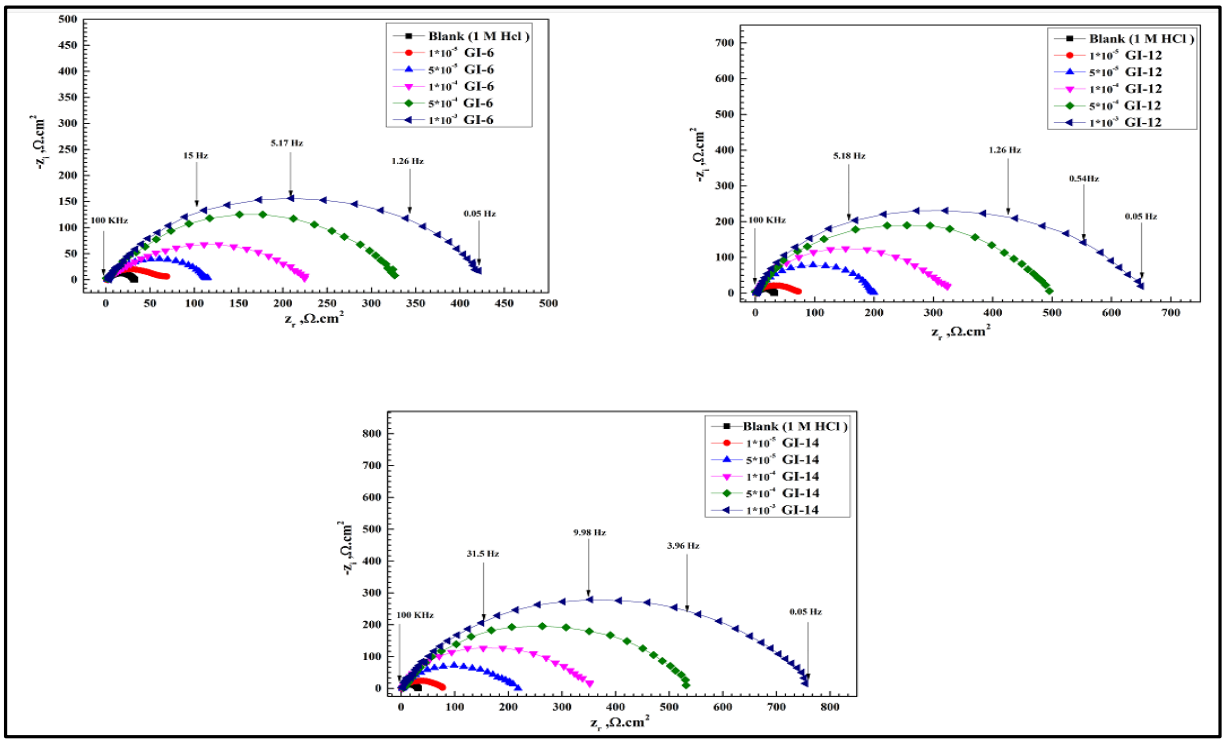

Fig. 8: Nyquist plots of X65-steel in 1.00 M HCl in the absence and presence of different concentrations of the prepared GI-surfactants (GI-6, GI-12, GI-14) at 298 ±1K.

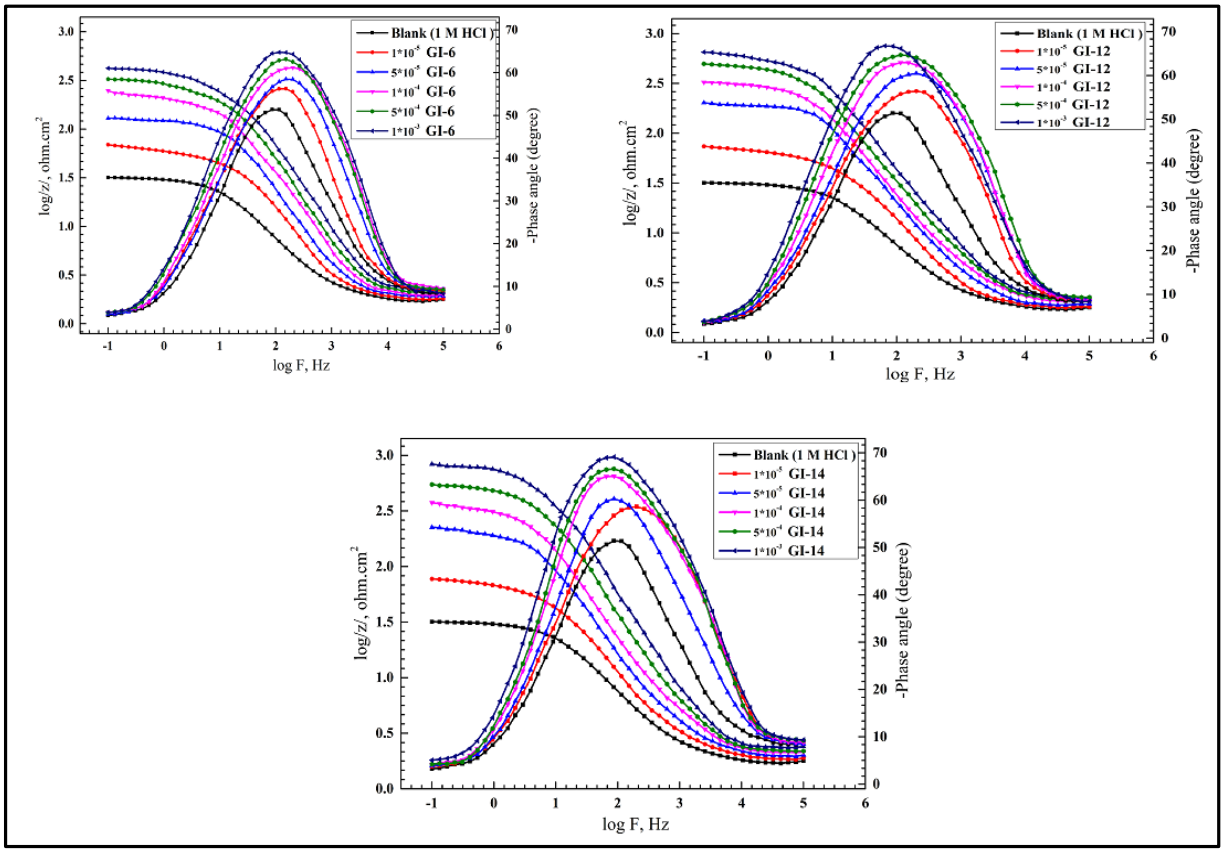

Fig. 9: Bode and phase degree diagrams for X65-steel in 1.00 M HCl in the absence and presence of different concentrations of the prepared GI-surfactants (GI-6, GI-12, GI-14) at 298 ±1K.

Fig. 10 inset represented the best equivalent circuit suggested to fit the EIS experimental data. It consisted of (R_s), solution resistance in series with (R_{ct}), charge transfer resistance which is parallel with (CPE), constant phase element. To obtain more fitted simulated data, CPE which had frequency dispersion could be replaced by the ideal (C_{dl}), double-layer capacitance [48]. The fitted EIS electrochemical data were recorded in Table 8. The impedance of CPE was pronounced by the next equation [18]:

$$Z_{CPE} = Q^{-1} (i\,\omega_{max})^{-n} \qquad (13)$$

where Q was the constant phase element constant, ω_{max} was the angular frequency, $\omega = 2\pi f_{max}$, (where f_{max} was the frequency at the highest imaginary element of the impedance), i was the imaginary quantity and n was a phase shift. Also, (C_{dl}) values could be determined according to the following equation and also tabulated in Table 8 [49]:

$$C_{dl} = 1/(2\pi R_{ct} F_{img \to Max}) \qquad (14)$$

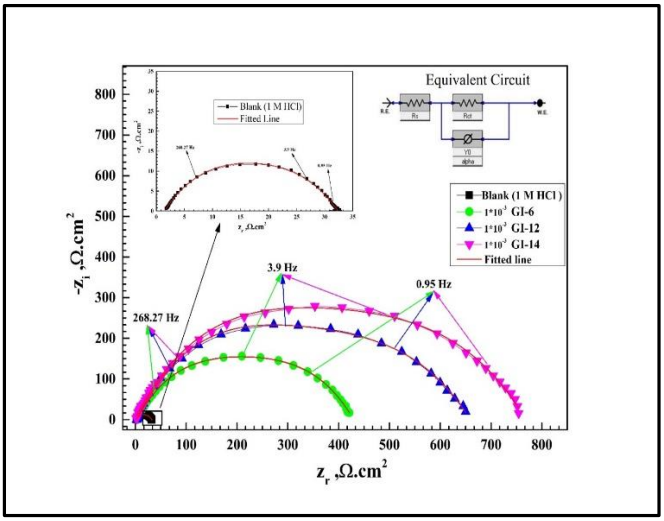

Fig. 10: Comparative the Nyquist plots for X65-steel in 1.00 M HCl in the absence and presence of 1x10^{-3} M concentrations of GI-surfactants (GI-6, GI-12, GI-14) at 298 ±1K. The equivalent circuit is inset.

Table (8): EIS parameters for X65-steel in 1 M HCl solution in the absence and presence of different concentrations of the prepared GI-surfactants at 298 ±1K.

Inh.	*Conc.(M)*	R_s *(ohm/cm^{-2})*	R_{ct} *(ohm/cm^{-2})*	*n*	C_{dl} *(Fcm^{-2}) x10^{-5}*	*IE %*
GI-6	***Blank***	*1.549*	*30.31*	*0.803*	*4.177*	---
	1x10^{-5}	*0.732*	*59.50*	*0.881*	*3.081*	*49.05*
	5x10^{-5}	*1.965*	*112.45*	*0.885*	*2.161*	*73.04*
	1x10^{-4}	*1.801*	*224.16*	*0.875*	*0.465*	*86.47*
	5x10^{-4}	*0.919*	*329.33*	*0.892*	*0.180*	*90.79*
	1x10^{-3}	*1.715*	*420.81*	*0.901*	*0.106*	*92.79*
GI-12	***1x10^{-5}***	*0.280*	*69.76*	*0.859*	*4.177*	*56.54*
	5x10^{-5}	*2.059*	*195.16*	*0.869*	*1.982*	*84.46*
	1x10^{-4}	*0.617*	*317.54*	*0.878*	*0.939*	*90.45*
	5x10^{-4}	*1.271*	*490.88*	*0.892*	*0.247*	*93.82*
	1x10^{-3}	*1.201*	*654.58*	*0.910*	*0.091*	*95.36*
GI-14	***1x10^{-5}***	*0.392*	*77.30*	*0.882*	*4.177*	*60.80*
	5x10^{-5}	*0.397*	*207.5*	*0.879*	*1.349*	*85.39*
	1x10^{-4}	*0.905*	*349.57*	*0.881*	*0.666*	*91.33*
	5x10^{-4}	*1.618*	*536.66*	*0.891*	*0.169*	*94.35*
	1x10^{-3}	*1.29*	*763.88*	*0.899*	*0.062*	*96.03*

After analysis of the tabulated results, the following outcomes were drawn:

I. R_{ct} values increased with the addition of GI-surfactants even in small concentrations. Furthermore, R_{ct} values related to alkyl chain length. The R_{ct} values have remarkably been improved due to the development of insulating protecting layer from surfactant molecules at the metal/electrolyte interface that reserved the X65-steel surface away from the aggressive action of the test solution [50].

II. At 1x10^{-3} M, the R_{ct} of inhibitor GI-14 (763.88 Ω cm^2) was more than those for GI-12 (654.58 Ω cm^2) or GI-6 (420.81 Ω cm^2). So, the inhibition capability of surfactant GI-14 in 1 M HCl was higher than other counterpart surfactants, and this was obtained in Fig. 10.

III. C_{dl} values dropped in the presence of the GI-surfactants due to replacement of water molecule or /and increase the electrical double layer thickness (T) on metal surface according to following Helmholtz model [50, 51]:

$$C_{dl} = (\varepsilon^0 \varepsilon / T)\, A \qquad (15)$$

where A was the surface area of the electrode used, ε◦ and ε were the permittivity of air and the local dielectric constant, respectively.

IV. The C_{dl} values are related to the subjected working electrode surface area. With the GI-surfactants' addition, the surface became almost covered with adsorbed GI-surfactants molecules and free to a slight extent from the corrosion products. This adsorption phenomenon led to increase of the smoothness of X65-steel surface.

V. The inhibition efficiency values increased by increasing GI-surfactants concentration and alkyl chain length touched the highest at optimum concentration (1x10^{-3} M) for all used

GI-surfactants; where it was 92.79, 95.36, and 96.03% for GI-6, GI-12, and GI-14, respectively.

Finally, the decrease in C_{dl} value was more pronounced at $1x10^{-3}$ M. Scientifically, the double layer between the charged metal surface and the solution is considered as an electrical capacitor. The adsorption of GI-surfactants molecules on the surface of X65-steel can influence its electrical capacity. This can be explained by the water molecules replacement with GI-surfactants molecules. Water molecules have dielectric constant higher than passive film formed on the metal surface. In fact, a decrease in C_{dl} in the presence of GI-surfactants proves the protective layer formation on the metal surface [52].The parameter n is another useful data showing surface roughness/ heterogeneity. Both metal surface degradation in HCl solution and the GI-surfactants molecules adsorption on the X65-steel surface can be studied by characterizing this parameter [53]. According to Table 8, the lowest value of n was observed for the sample immersed in 1 M HCl solution with $1x10^{-5}$ M. It is clear from Table 8 that addition of GI-surfactants up to $1x10^{-5}$ M caused a decrease in n value. It has been found that inhibitors could reduce surface damage and roughness of metals in acidic solution resulting in an increase in n value. Therefore, the decrease observed for n value in this study cannot be attributed to a decrease in metal surface damage. This may be attributed to the surface inhomogeneity arising from non-uniform film formation on the metal surface. The random adsorption of GI-surfactants molecules on the metals surface (both vertical and parallel to the metal surface) may be responsible for a decrease in surface homogeneity. The inhomogeneity increased at higher GI-surfactants concentration [54].

3.7. Potentiodynamic polarization measurements (PDP)

PDP curves of X65-steel immersed in 1M hydrochloric acid solution free and even after adding dissimilar concentrations of the synthesized GI-surfactants at 298 ±1K have been shown in Fig. 11. The corresponding electrochemical indices, such as corrosion potential (E_{corr}), specific corrosion current density (i_{corr}), cathodic and anodic Tafel slopes (β_c , β_a), polarization resistance (R_p) and the percent of inhibition efficiency (IE %) were computed and presented in Table 9. Moreover, R_p values were calculated from the following Stern-Geary Equation and its values were tabulated in Table 9 [55]:

$$R_p = \beta_a\beta_c/2.303\, i_{corr}\,(\beta_a + \beta_c\,) \qquad (16)$$

Close inspection of the curves of Fig. 11 and the kinetic parameters reported in Table 9 were shown and discussed as follow:

I. Tafel lines were shifted in more noble direction compared to the blank one. This inferred that the hydrogen evolution and dissolution reactions of X65-steel have been inhibited.
II. There is no remarkable shift in E_{corr} as a result of adding GI-surfactants. Based on these results, the prepared inhibitors act as mixed-type [56]. Thus, the adsorption process on the steel surface could take place by blocking both anodic and cathodic sites of X65-steel corrosion [57].
III. The i_{corr} values depend on the inhibitors molecular weight and its concentration [58]. The i_{corr} values decreased by increasing both of the surfactant's concentration and the sum of carbon atoms in the hydrophobic chain of GI-surfactants. The lowering in the value of i_{corr} was an indication of increasing the inhibition effect of the prepared GI-surfactants. Also, R_p values were inversely proportional to i_{corr} values. So, an increasing in R_p values could be obtained by increasing the concentration of the added surfactants due to the film adsorbed on X65-steel surface which increased the corrosion resistance reaction.
IV. According to Fig. 11, cathodic Tafel lines were quite parallel which designated that, the hydrogen reduction process was activated and controlled [59].
V. From the anodic Tafel lines obtained in Fig. 11, the phenomena of desorption were prominent at elevated anodic potential above -0.220 mV Vs E_{ocp}, in which the adsorption rate of GI-surfactants was lower than their desorption rate. Unlike GI-surfactants molecules at low anodic potential less than -0.220 mV Vs E_{ocp} favor adsorption than desorption as a result of its dependence on its concentration hence forming permanent protective layer over X65-steel surface [60].

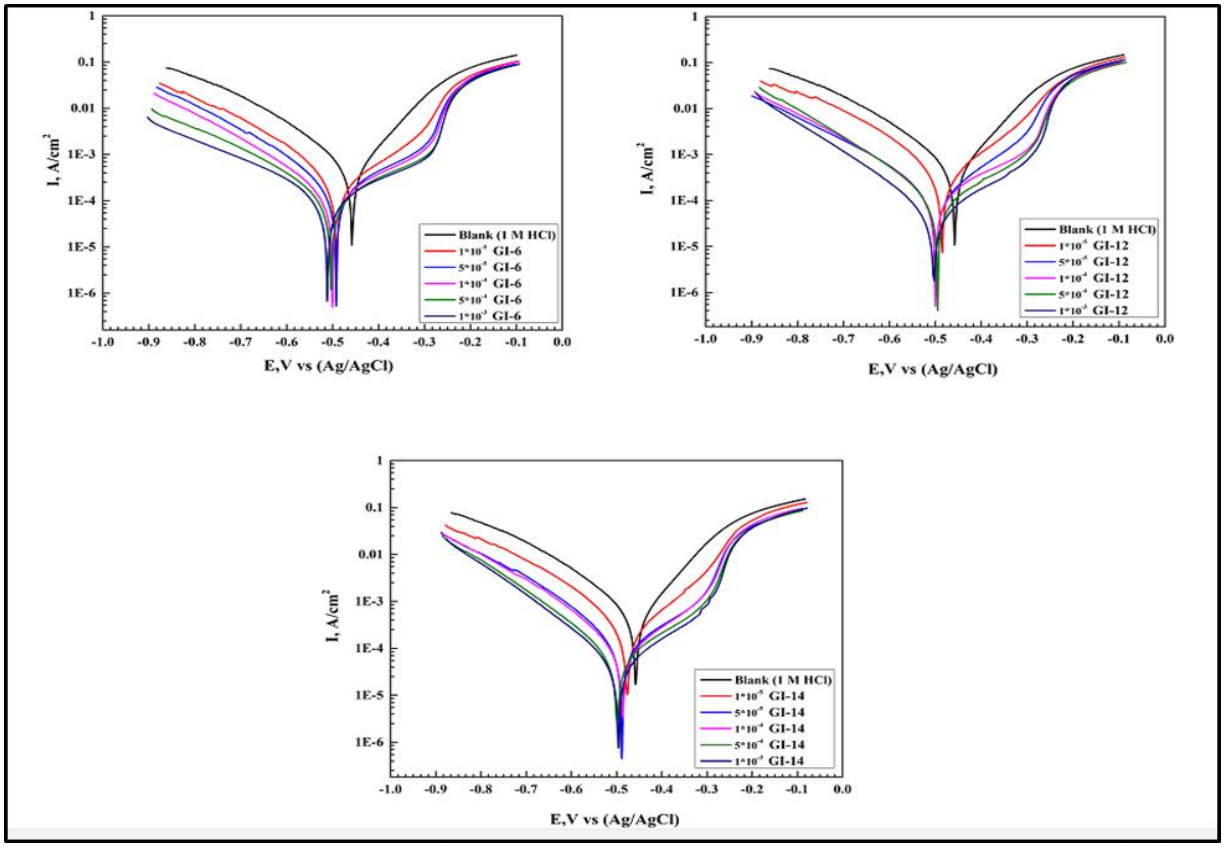

Fig 11: Cathodic and Anodic polarization curves for X65-steel in 1.00 M HCl obtained at 298 ±1K in the absence and presence of different concentrations of the prepared GI-surfactants (GI-6, GI-12, GI-14).

VI. Increasing the values of IE % by increasing the concentration of GI-surfactants indicated that, the adsorption of the prepared surfactants on X65-steel surface reduced the area exposed to HCl and hence, decreased the X65-steel corrosion reaction. This reflected the inhibitory action of the used GI-surfactants towards the X65-steel corrosion in 1M HCl.

VII. At optimum concentration ($1x10^{-3}$ M), IE % increased in the order: GI-14 > GI-12 > GI-6, which was the same order previously reported using the EIS and weight loss technique at 298 K. This could be attributed to the presence of number of electrons donating centers in tested corrosion inhibitor (N) and π-bond. In addition, the carbon chains of the surfactant inhibitor molecules enhance stronger protective adsorption film, preventing the aggressive chloride ions to interact with steel surface.

Table 10, showed the superiority of our prepared compound (GI-14) compared to the published work

Table (9): polarization parameters for X65-steel in 1 M HCl solution in the absence and presence of different concentrations of the prepared GI-surfactants at 298 ±1K.

3.8. Morphology studies

The morphological changes occurred on X65-steel surface treated and untreated with ($1x10^{-3}$ M) in 1M HCl of GI-14 surfactant after 6*h* immersion was studied by SEM (Fig. 12a and b). The elemental analysis studies of X65-steel outer layer were done using EDX (Fig. 13 a and b). The X65-steel surface in contact directly with blank HCl appeared rougher and strongly damage due to metal dissolution (Fig. 12a).

under the same conditions[61-65]. The obtained results were in a good agreement with the EIS measurements. Take into consideration, R_P values were almost closed to those of the R_{ct}. From the aforementioned results we noted that, the investigational data were reliable and matched with each other.

Table (10): Comparison between the corrosion inhibition efficiency of the prepared (GI-14) surfactant and some other reported inhibitor for Fe-alloys in acidic media.

Inh.	medium	Conc.	IE%	method	Ref.
GI-14	**1M HCl**	**$1x10^{-3}$**	**96**	**PDP**	**this study**
(SCGS)		$1x10^{-3}$	95.57	PDP	[61]
Gemini surfactant		$1x10^{-3}$	96.13	PDP	[62]
Cationic Surfactant (II)		$5x10^{-3}$	93.8	PDP	[63]
Gemini surfactant (III)		$1x10^{-3}$	92.96	PDP	[64]
IL6		$5x10^{-3}$	93	PDP	[65]

Inh.	Conc. (M)	$-E_{corr}$, (V) Ag/AgCl	i_{corr} (A/cm^2) $x10^{-4}$	β_a (V/dec)	$-\beta_c$ (V/dec)	CR (mm/year)	R_P (Ω)	IE %
GI-6	Blank	0.439	8005	0.1112	0.1860	9.301	37.76	---
	$1x10^{-5}$	0.462	4013	0.1271	0.1705	4.662	78.85	49.87
	$5x10^{-5}$	0.492	1956	0.1852	0.1742	2.005	225.86	75.56
	$1x10^{-4}$	0.500	1543	0.1889	0.1419	1.677	243.81	80.71
	$5x10^{-4}$	0.503	1000	0.1870	0.1451	1.510	360.41	87.51
	$1x10^{-3}$	0.511	0.590	0.1871	0.1424	1.243	458.69	92.63
GI-12	$1x10^{-5}$	0.485	3174	0.1113	0.1570	3.688	89.12	60.34
	$5x10^{-5}$	0.501	1372	0.1208	0.1747	1.595	225.98	82.85
	$1x10^{-4}$	0.502	1012	0.1928	0.1267	1.177	327.97	87.35
	$5x10^{-4}$	0.495	0.570	0.0957	0.0800	0.552	499.6	92.88
	$1x10^{-3}$	0.502	0.390	0.1647	0.1436	0.440	701.1	95.13
GI-14	$1x10^{-5}$	0.476	2881	0.1137	0.1864	3.348	106.49	64.00
	$5x10^{-5}$	0.488	1267	0.1402	0.1806	1.472	270.53	84.16
	$1x10^{-4}$	0.487	0.799	0.1493	0.1319	0.929	380.44	90.00
	$5x10^{-4}$	0.498	0.510	0.1661	0.139	0.677	565.29	93.62
	$1x10^{-3}$	0.496	0.310	0.1594	0.1295	0.462	780.83	96.12

However, adding GI-14 impeded the corrosion of X65-steel, giving a smoother surface (Fig. 12b). This ensured the formation of a protective passive film layer of GI-14 molecules over X65-steel surface [66]. Furthermore, the elemental analysis spectra using EDX showed the chemical composition of the external layer of X65-steel surface subjected to HCl and after using ($1x10^{-3}$ M) GI-14 surfactant as exist in Fig. 13 a and b. EDX spectrum of blank (untreated) X65-steel sheet characterized by the high-intensity peaks of chloride and oxygen. This confirmed the formation of corrosion products (iron chloride, oxide, and hydroxides) over the X65-steel surface due to the highly offensive action of HCl. On the other hand, the disappearance of chloride peak and low oxygen intensity one indicated the lowering corrosion rate of X65-steel. Furthermore, the appearance of N-peak and enhancing the intensity peaks of Carbone and iron in compared with EDX spectra of blank X65-steel supported the suggested postulation of adsorbed layer formation from GI-surfactants compounds over the X65-steel surface. These observations were matched with the previously published paper [67]. These results were in good agreement with WL, PDP, and EIS measurements revealed above.

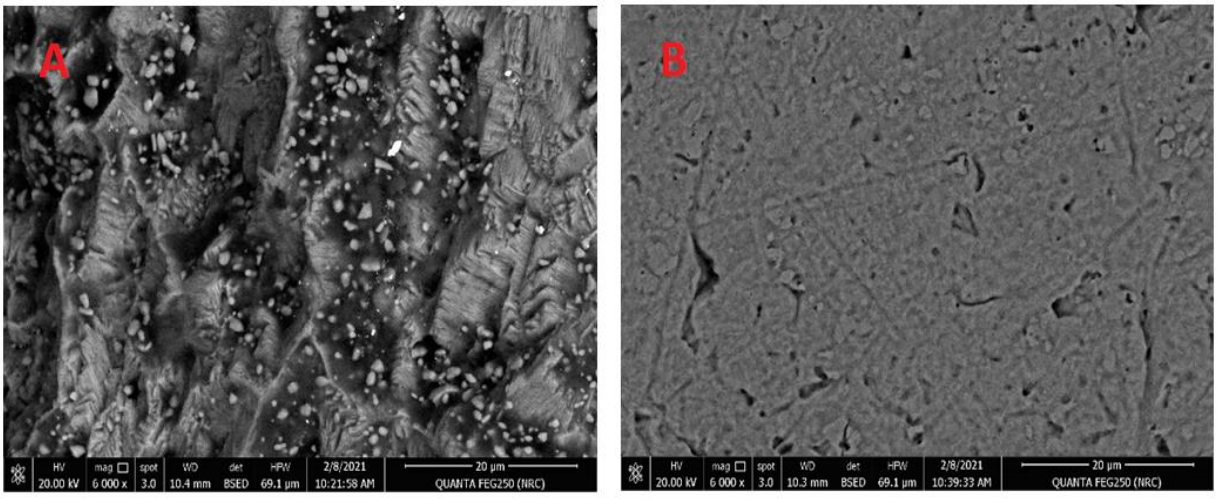

Fig. 12: SEM for the X65-steel surface: (A) sample immersed in (1.00) M HCl, (B) sample immersed in (1.00) M HCl treated with ($1x10^{-3}$) of GI-14 surfactant.

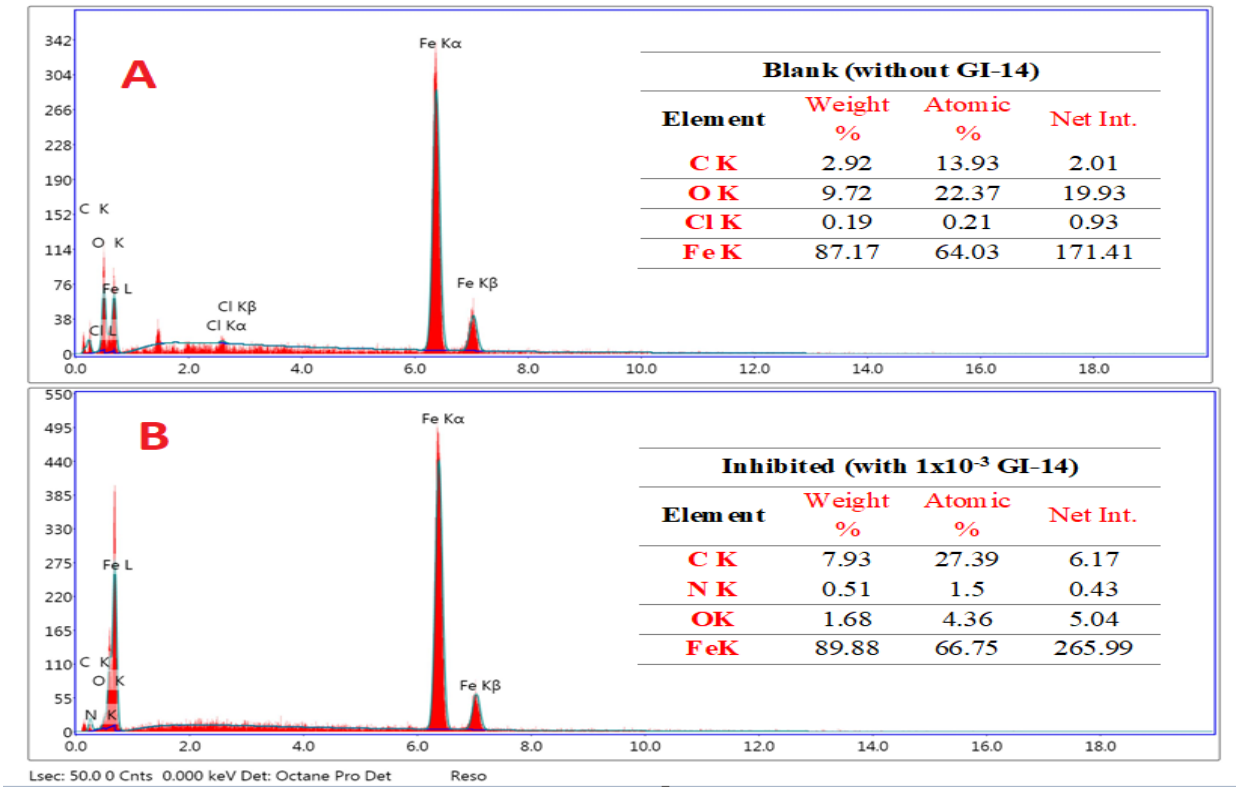

Fig. 13: EDX for the X65-steel surface: (A) sample immersed in (1.00) M HCl acid solution without GI-14 surfactant, (B) sample immersed in (1.00) M HCl acid solution with ($1x10^{-3}$) of GI-14 surfactant.

3.9. Computational indices

Computational studies were considered as an important way to show the chemical reactivity of the prepared GI-surfactants and to pronounce their corrosion inhibition reaction mechanism established based on the donor-acceptor interaction concept [68]. Based on DFT theory, the relation between the inhibition efficiency of the organic molecules and their molecular/electronic structure could be deliberated. Based on frontier molecular orbital theory (FMOT), the electron density was distributed over the optimized structures in gas and solvent phases as HOMO, LUMO, electron density, and molecular electrostatic potential (MEP) mapping which were obtained in Fig. 14 and Fig. 15. The prepared GI-surfactants had a polar head including lone pair of electrons in heteroatoms (N) and delocalization of π-electrons in the benzylidene rings and imine group in which the electron density focused on them, demonstrating that these locations were the adsorption active sites, which increased the polarity of the molecule, increasing the adsorption possibility and averting surface interactions with the corrosive media. According to the molecular electrostatic potential (MEP) mapping of the insight compounds, as illustrated in Fig. 14 and Fig. 15, the red region (N atoms and π-electrons phenyl) is considered the nucleophilic center for adsorption, improving the opportunity of the adsorption procedure, establishing a shielding layer on the metal surface, hence increasing the inhibition efficiency. Also, the electron density distributed over the whole molecule increased the adsorption intensity of molecule over X65-steel surface which caused the aggressive chloride anions away from the surface. The hydrophobic carbon chain supported the adherence of adsorbed molecules.

The corresponding numerical values of quantum chemical parameters of the prepared GI-surfactants (GI-6, GI-12, and GI-14) in the gas and solvent phases containing the energies of HOMO (ev), LUMO (ev), the energy gap (ΔE), electron affinity (A), ionization potential (I), global hardness (η) and electronegativity (χ) were calculated as per the following equations along with their corresponding quantum chemical parameters, (Table 11) [69] :

$$I = -E_{\mathrm{HOMO}} \quad (17)$$

$$A = -E_{\mathrm{LUMO}} \quad (18)$$

$$\eta = \frac{\Delta E_{\mathrm{gap}}}{2} \quad (19)$$

$$\chi = \frac{-(E_{\mathrm{HOMO}} + E_{\mathrm{LUMO}})}{2} \quad (20)$$

E_{HOMO} and E_{LUMO} were responsible for the electron shearing between GI-surfactants and X65-steel 3d orbitals [70]. From Table 11 the values of E_{LUMO} and E_{HOMO} decreased and increased respectively by increasing the alkyl chain length in the investigated GI-surfactants. From the data obtained in Table 11 in the gas phase, GI-14 had a higher E_{HOMO} value (-7.081eV) and lower E_{LUMO} value (-1.16 eV) than those of GI-12 and GI-6. So, it could be said that the GI-14 surfactant can easily give electrons to an unoccupied molecular orbital. This substantially enhanced its adsorption effect more than GI-12 and GI-6 [71]. On the other hand, the energy gap values ΔE_{gap} can control the chemical reactivity [25]. From this point, the lower ΔE_{gap} values, the higher chemical reactivity which gave good inhibition properties owing to the small excitation energy required for an electron to be promoted. Therefore, GI-14 surfactant gave a more stable adsorption form with the X65-steel than GI-12 and GI-6. On the other hand, according to the Lewis acid/base theory, soft molecules were generally more active compared to hard ones. The lower the ΔE value, the softer the molecule will be and vice versa is right [68]. Table 11 showed that GI-14 had the lowest hardness value. Ionization potential was another parameter that expressed the chemical reactivity of the molecules. Smaller values of ionization energy indicated higher reactivity of the atoms and molecules, in contrast to large values that showed high stability of the molecules [72]. From Table 11, the low ionization energy value indicated the high inhibition efficiency of GI-14. An additional significant quantum parameter that was used to affirm the relationship between the efficiency of the prepared GI-surfactants and its electron-donating capability to/or from the X65-steel was the number of electron transfers (ΔN). ΔN could be intended according to the following equation [73]:

$$\Delta N = \frac{(\chi_{Fe} - \chi_{inh.})}{2(\eta_{Fe} + \eta_{inh.})} \quad (21)$$

where, $\chi_{inh.}$ and χ_{Fe} represented the absolute electronegativity of surfactant molecule and steel (7 eV/mol), respectively, $\eta_{inh.}$ and η_{Fe} represented the absolute hardness of surfactant molecule and steel (0 eV/mol), respectively [73]. The tendency of providing electrons to the steel surface increased by increasing ΔN values when the value of calculated ΔN were less than 3.6 [74]. From Table 11, the values of ΔN for the GI-surfactants progressed in the order: GI-14> GI-12> GI-6 in the gas and solvent phase. Therefore, the GI-14 compound had the maximum ability to supply electrons to the X65-steel surface. The inhibition efficiency values obtained from the experimental techniques used and E_{HOMO} values of the prepared GI-surfactants were in agreement.

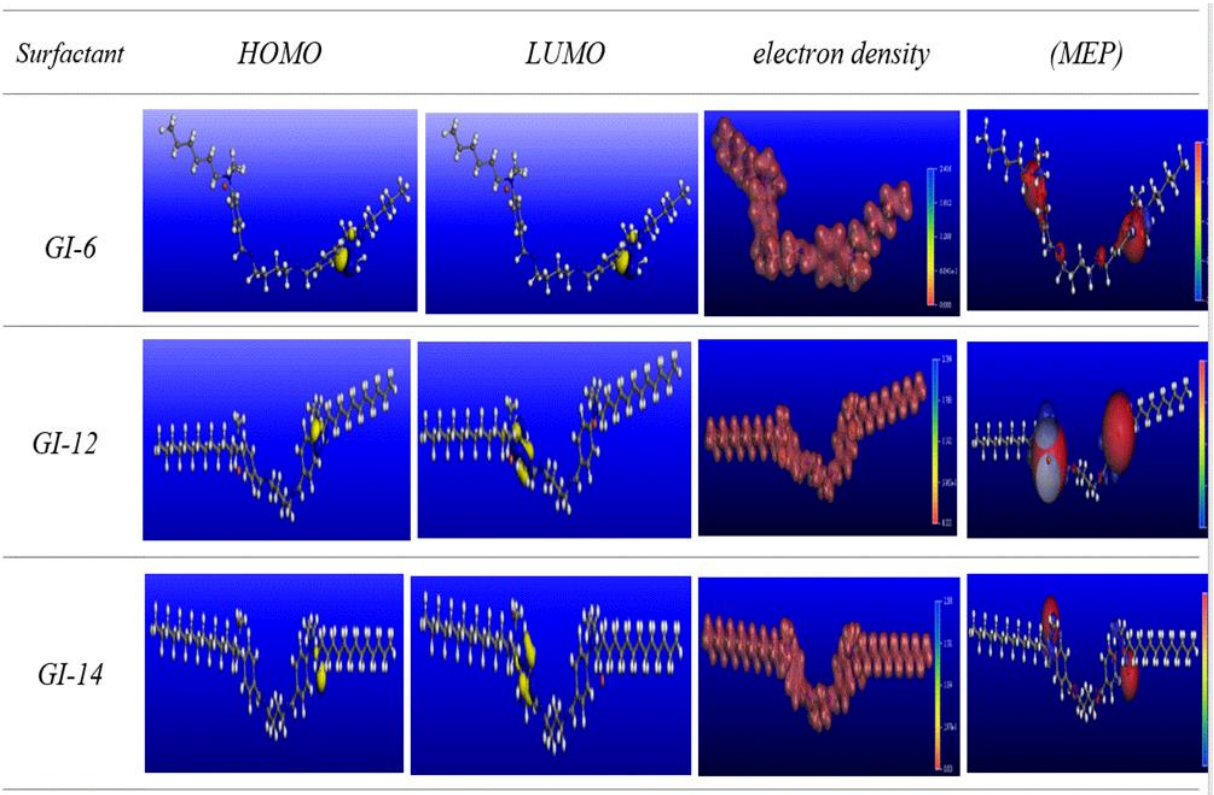

Fig 14: The (HOMO), (LUMO) total occupation, total electron density, and molecular electrostatic potential (MEP) mapping distribution for the investigated GI-surfactants GI-6, GI-12, and GI-14 in the gas phase.

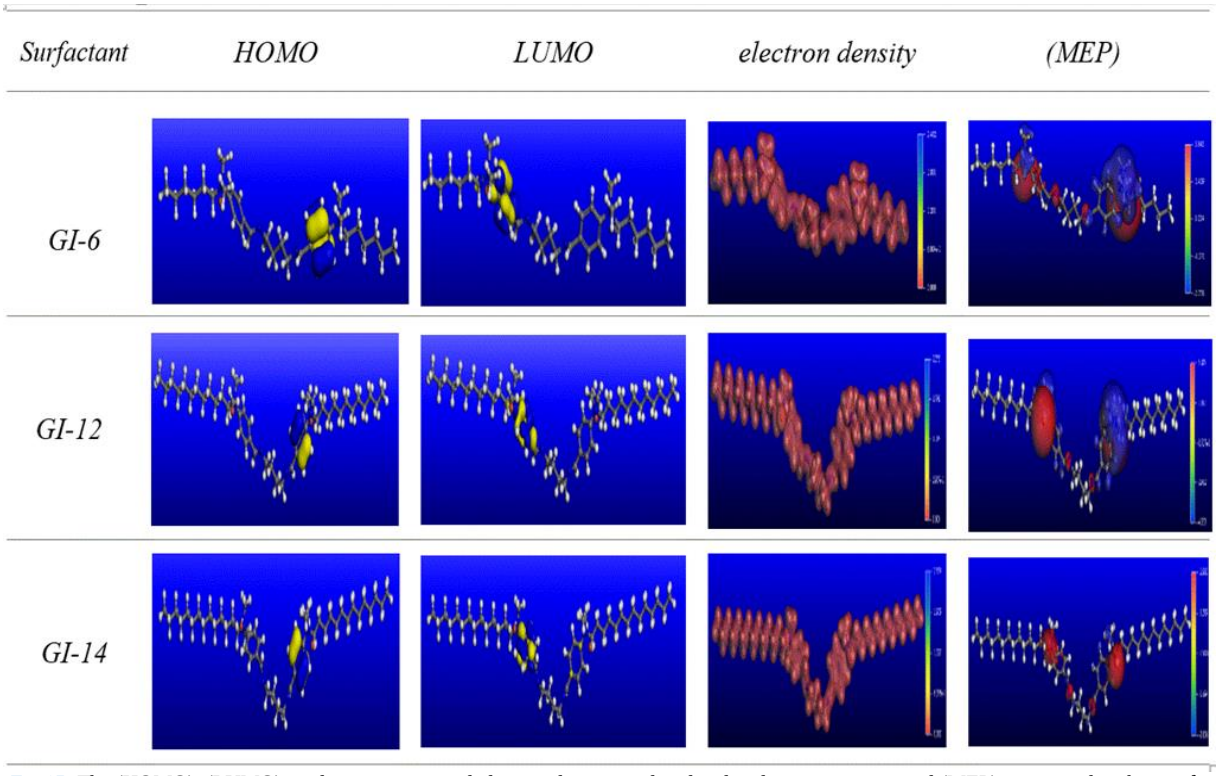

Fig 15: The (HOMO), (LUMO) total occupation, total electron density, and molecular electrostatic potential (MEP) mapping distribution for the investigated GI-surfactants GI-6, GI-12, and GI-14 in solvent phase.

Table (11): Quantum chemical calculated parameters of the investigated GI-surfactants.

Phase	Inh.	E_{HOMO} (eV)	E_{LUMO} (eV)	ΔE (eV)	A (eV)	I (eV)	X (eV)	η (eV)	ΔN
Gas	GI-6	-7.101	-1.133	5.968	1.133	7.101	4.117	2.984	0.4831
	GI-12	-7.092	-1.135	5.957	1.135	7.092	4.114	2.979	0.4846
	GI-14	-7.081	-1.16	5.921	1.16	7.081	4.121	2.961	0.4863
Solvent	GI-6	-9.954	-0.741	9.213	0.741	9.954	5.348	4.607	0.1794
	GI-12	-9.952	-0.741	9.211	0.741	9.952	5.347	4.606	0.1795
	GI-14	-9.951	-0.742	9.209	0.742	9.951	5.347	4.605	0.1796

3.10. Monte Carlo simulation (MCs)

MCs method was considered a very helpful tool that expected the performance and the interaction between the adsorbed GI-surfactants over the metallic surface; Fe surface to maximize the benefits output from the DFT data. The MCs for the prepared GI-surfactants (GI-6, GI-12, and GI-14) in the gas phase and solvent simulated with 200 H_2O were geometry-optimized to simulate the real corrosive medium which had been executed using adsorption locator module. Side and top views (Snapshots) for the optimized GI-surfactants in gas and solvent phases over Fe (1 1 0) cleaved surface were presented in Fig. 16, and 17 respectively. It was obvious that Side views snapshots of the optimized structure appeared with a parallel orientation of the prepared GI-surfactants on the Fe (1 1 0) surface. This, in turn, led to their strong interaction possibility with Fe (1 1 0) surface [75]. On the other hand, top views snapshots of the optimized structure appeared the prepared surfactant molecules covered a high surface area of the steel surface.

The outputs of the simulation method were recorded in Table 12. The negative values of E_{ads} in gas and solvated phases designate the spontaneous adsorption process of the tested compound and their absolute values indicated the higher and strong adsorption affinity of the prepared GI-surfactants on the metal surface. All the numerical values obtained in the gas and solvent phases, Table 12, indicated that the adoption energy in the case of the solvent phase was higher than their counterparts in the gaseous phase which was associated with intermolecular H-B interactions between GI-surfactants and water

molecules that enhanced their adsorption on the steel surface and this matched with the previous published paper [76]. Adsorption energy values indicated the order of adsorption ability of the tested compounds GI-6 < GI-12 < GI-14 and this matched with experimental data obtained.

Table (12): The outputs energies were calculated by Monte Carlo simulation for the investigated GI-surfactants in gas and simulated acid solution phases on Fe (1 1 0).

Surfactant		E_T (KJ/mol)	E_{ads} (KJ/mol)	$E_{rig.ads}$ (KJ/mol)	$E_{def.}$ (KJ/mol)
GI- 6	gas	-424.96	-395.28	-303.26	-92.02
	200 H_2O	-3439.14	-4501.40	-3311.21	-1190.19
GI-12	gas	-541.24	-545.37	-514.77	-30.60
	200 H_2O	-3479.86	-4594.52	-3314.46	-1180.05
GI-14	gas	-630.41	-553.126	-462.80	-90.32
	200 H_2O	-3587.45	-4679.78	-3568.37	-1111.41

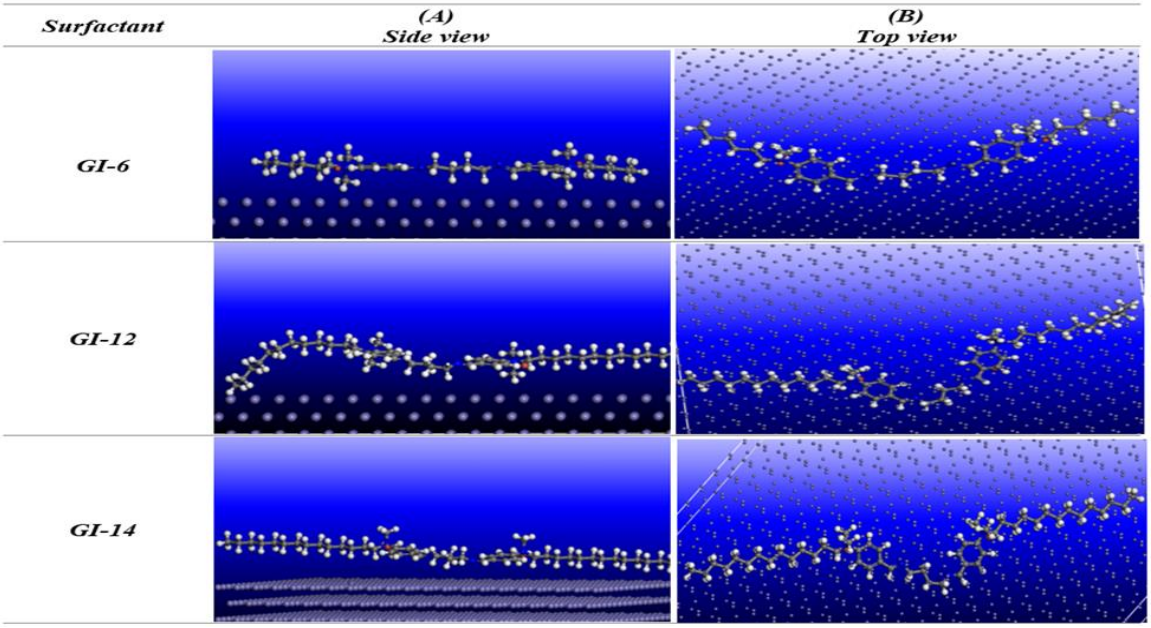

Fig. 16: Side and top views of the adsorption mode of the investigated GI-surfactants GI-6, GI-12 and GI-14 in gas phase on Fe (1 1 0) substrate.

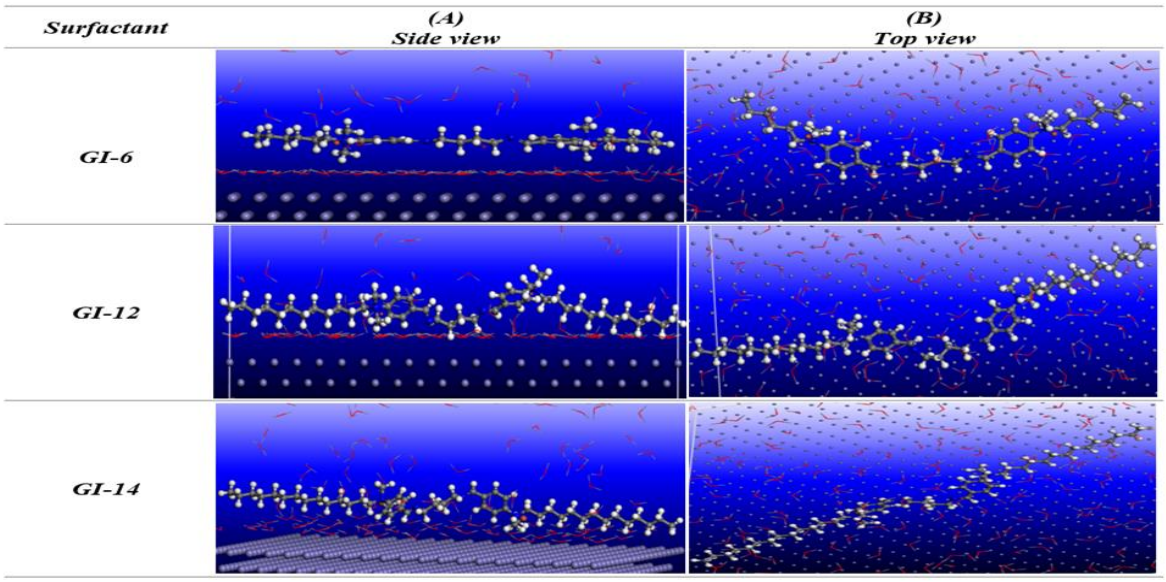

Fig. 17: Side and top views of the adsorption mode of the investigated GI-surfactants GI 6, GI-12, and GI-14 in solvent phase on Fe (1 1 0) substrate.

3.11. Mechanism of inhibition

Usually, the adsorption of organic inhibitors on the metal surface is influenced by the presence of donor atoms, the molecular structure, the type of the aggressive solution, the nature, and the charge present on the metal surface. All the investigated compounds in this study have quaternary nitrogen N^+, counter ion (Br^-), imine (–C=N–) functional group(s), and π - electrons in the aromatic rings. These groups were considered as the active center for the adsorption process which was affected by the type of interaction between the metal surface and inhibitor molecules. According to section (3.6), the inhibition process occurred by blocking mechanism on cathodic and anodic areas of the metal surface (inhibit both anodic and cathodic reactions) [77]. In this case, the quaternary nitrogen atom (N^+) is adsorbed at the cathodic site to reduce hydrogen evolution. At the anodic site, the counter ion (Br), π-electrons of the aromatic ring, and the lone pair electrons of the imine group (–C=N–) are adsorbed to decrease the anodic dissolution of the X65-steel. More precisely, the interaction between inhibitor (GI-14) as a representative compound and the X65-steel surface was suggested in Fig. 18. There are two uppermost adsorption methods between the GI-14 surfactant molecule and the X65-steel surface: first, electrostatic interaction via the quaternary (N^+) and counter ion (Br^-) on surfactant molecule with the negatively Cl^- ions (produced from medium) and Fe^+ ions, respectively. This kind of interaction between them represented physical adsorption. Second, the chemical coordination type involved the sharing of electrons between lone pairs on nitrogen and unoccupied d-orbitals on ionized iron atom and hence represented chemical adsorption. Along with this the interaction between delocalized electrons on surfactant aromatic ring and ionized iron represented retro-donation. Finally, the presence of a large alkyl chain length in surfactant (GI-14) compared to other surfactants (GI-12 and GI-6) made the head groups more directed to the metal surface and so possess more inhibition ability. The above discussion was also in agreement with experimental ΔG°_{ads} values i.e., mixed type of adsorption.

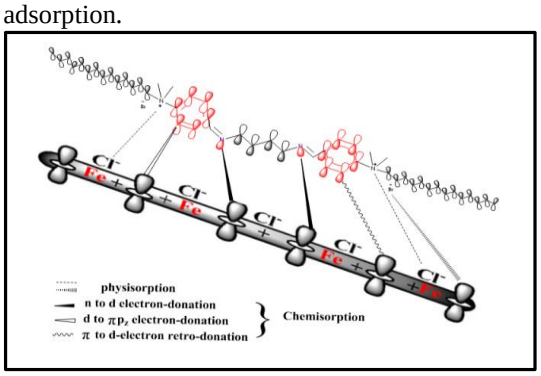

Fig. 18: Suggested adsorption model of the as-prepared GI-14 surfactant over the X-65 steel.

4. Conclusion

Based on the results of the investigation, the following conclusions were drawn:

1. GI-surfactants used here were found good inhibitors for X65-steel corrosion in 1 M HCl with relatively high efficiencies.
2. The IE% increased by increasing the inhibitor concentration but decreased by increasing the temperature. The IE% increase in the order: GI-14 > GI-12 > GI-6.
3. The prepared GI-surfactants exhibited good surface active properties.
4. The experimental measurements using the WL method ensured the adsorption of GI-surfactants on the iron surface which obeyed the Langmuir isotherm. The K_{ads} follow the order: GI-14 > GI-12 > GI-6.
5. Polarization results showed that the three GI-surfactants acted as mixed-type inhibitors.
6. EIS spectra exhibited one capacitive loop i.e., corrosion of X65-steel was controlled by charge transfer in which, the presence of GI-surfactants in 1 M HCl solution increased R_{ct} while reduced C_{dl}.
7. Monte Carlo simulation results indicated that the prepared GI-surfactants highly bind on the X65-steel surface utilizing the lone pair of electrons on the heteroatoms as well as the π-electrons in the benzylidene rings.
8. These outcomes are well evidenced quantitatively by EDX measurements.
9. Experimental and theoretical analysis data suggest the validity of these compounds to be among of the more applicable compounds in corrosion mitigation filed such as, acidizing, acid cleaning jobs.

5. Conflicts of interest

"There are no conflicts to declare".

6. Formatting of funding sources

"There are no funding sources".

Acknowledgments

The authors gratefully thank the Egyptian Petroleum Research Institute and Al-Azhar University for their supports

7. References

[1] M. Lagrenee, B. Mernari, M. Bouanis, M. Traisnel, F. Bentiss, Study of the mechanism and inhibiting efficiency of 3, 5-bis (4-methylthiophenyl)-4H-1, 2, 4-triazole on mild steel corrosion in acidic media, Corrosion Science 44(3) (2002) 573-588.

[2] E.A. Badr, Inhibition effect of synthesized cationic surfactant on the corrosion of carbon steel in 1 M HCl, Journal of Industrial and Engineering Chemistry 20(5) (2014) 3361-3366.

[3] K. Ramya, A. Joseph, Dependence of temperature on the corrosion protection properties of vanillin and

its derivative, HMATD, towards copper in nitric acid: theoretical and electroanalytical studies, Research on Chemical Intermediates 41(2) (2015) 1053-1077.
[4] S. Javadian, A. Yousefi, J. Neshati, Synergistic effect of mixed cationic and anionic surfactants on the corrosion inhibitor behavior of mild steel in 3.5% NaCl, Applied Surface Science 285 (2013) 674-681.
[5] I. Zaafarany, M. Abdallah, Ethoxylated fatty amide as corrosion inhibitors for carbon steel in hydrochloric acid solution, Int J Electrochem Sci 5(1) (2010) 18-28.
[6] Q. Zhang, Z. Gao, F. Xu, X. Zou, Adsorption and corrosion inhibitive properties of gemini surfactants in the series of hexanediyl-1, 6-bis-(diethyl alkyl ammonium bromide) on aluminium in hydrochloric acid solution, Colloids and Surfaces A: Physicochemical and Engineering Aspects 380(1-3) (2011) 191-200.
[7] Q. Zhao, Z. Gao, Synthesis and surface-active property of bis-quaternary ammonium-sodium sulfate Gemini surfactant, Frontiers of Chemistry in China 1(4) (2006) 434-437.
[8] W.W. Focke, N.S. Nhlapo, E. Vuorinen, Thermal analysis and FTIR studies of volatile corrosion inhibitor model systems, Corrosion science 77 (2013) 88-96.
[9] M. Hegazy, R. Samy, A. Labena, M.A. Wadaan, W.N. Hozzein, 4, 4′-(((1E, 5E)-pentane-1, 5-diylidene) bis (azanylylidene)) bis (1-dodecylpyridin-1-ium) bromide as a novel corrosion inhibitor in an acidic solution (part I), Materials Science and Engineering: C 110 (2020) 110673.
[10] S.M. Tawfik, Ionic liquids based gemini cationic surfactants as corrosion inhibitors for carbon steel in hydrochloric acid solution, Journal of Molecular Liquids 216 (2016) 624-635.
[11] D. Asefi, M. Arami, N.M. Mahmoodi, Electrochemical effect of cationic gemini surfactant and halide salts on corrosion inhibition of low carbon steel in acid medium, Corrosion Science 52(3) (2010) 794-800.
[12] M. Hegazy, A novel Schiff base-based cationic gemini surfactants: synthesis and effect on corrosion inhibition of carbon steel in hydrochloric acid solution, Corrosion Science 51(11) (2009) 2610-2618.
[13] H.M. Abd El-Lateef, M.A. Abo-Riya, A.H. Tantawy, Empirical and quantum chemical studies on the corrosion inhibition performance of some novel synthesized cationic gemini surfactants on carbon steel pipelines in acid pickling processes, corrosion Science 108 (2016) 94-110.
[14] M.J.C.S. Hegazy, A novel Schiff base-based cationic gemini surfactants: synthesis and effect on corrosion inhibition of carbon steel in hydrochloric acid solution, 51(11) (2009) 2610-2618.
[15] A. Badawi, M. Hegazy, A. El-Sawy, H. Ahmed, W.J.M.C. Kamel, Physics, Novel quaternary ammonium hydroxide cationic surfactants as corrosion inhibitors for carbon steel and as biocides for sulfate reducing bacteria (SRB), 124(1) (2010) 458-465.
[16] A.A. Abd-Elaal, N. Elbasiony, S.M. Shaban, E.J.J.o.M.L. Zaki, Studying the corrosion inhibition of some prepared nonionic surfactants based on 3-(4-hydroxyphenyl) propanoic acid and estimating the influence of silver nanoparticles on the surface parameters, 249 (2018) 304-317.
[17] M. Yadav, U. Sharma, P. Yadav, Isatin compounds as corrosion inhibitors for N80 steel in 15% HCl, Egyptian Journal of Petroleum 22(3) (2013) 335-344.
[18] A. El-Tabei, A.E. El-Tabey, N.J.A.S.S. El Basiony, Newly imine-azo dicationic amphiphilic for corrosion and sulfate-reducing bacteria inhibition in petroleum processes: Laboratory and theoretical studies, 573 (2022) 151531.
[19] M.M. Megahed, M.M. Abdel Bar, A.M. El-Shamy, Polyamide coating as a potential protective layer against corrosion of iron artifacts, Egyptian Journal of Chemistry 64(10) (2021) 3-4.
[20] A.M. El-Shamy, Fabrication of commercial nanoporous alumina by low voltage anodizing, Egyptian Journal of Chemistry 61(1) (2018) 175-185.
[21] Y. Reda, H. Yehia, A. El-Shamy, Microstructural and mechanical properties of Al-Zn alloy 7075 during RRA and triple aging, Egyptian Journal of Petroleum 31(1) (2022) 9-13.
[22] E. El-Kashef, A.M. El-Shamy, A. Abdo, E.A. Gad, A.A. Gado, Effect of magnetic treatment of potable water in looped and dead end water networks, Egyptian Journal of Chemistry 62(8) (2019) 1467-1481.
[23] K. Zohdy, A. El-Shamy, A. Kalmouch, E.A. Gad, The corrosion inhibition of (2Z, 2′ Z)-4, 4′-(1, 2-phenylene bis (azanediyl)) bis (4-oxobut-2-enoic acid) for carbon steel in acidic media using DFT, Egyptian journal of petroleum 28(4) (2019) 355-359.
[24] K. Khaled, N. Hackerman, Investigation of the inhibitive effect of ortho-substituted anilines on corrosion of iron in 1 M HCl solutions, Electrochimica Acta 48(19) (2003) 2715-2723.
[25] N. El Basiony, E.E. Badr, S.A. Baker, A.J.A.S.S. El-Tabei, Experimental and theoretical (DFT&MC) studies for the adsorption of the synthesized Gemini cationic surfactant based on hydrazide moiety as X-65 steel acid corrosion inhibitor, 539 (2021) 148246.
[26] A. Al-Sabagh, N. Nasser, N.G. Kandile, M. Migahed, A new family of surfactants: Part I: Synthesis of ethoxylated monoalkyl bisphenol and their investigation as corrosion inhibitiors, Journal of dispersion science and technology 29(2) (2008) 161-170.
[27] M. Hegazy, A. El-Etre, M. El-Shafaie, K.J.J.o.M.L. Berry, Novel cationic surfactants for

corrosion inhibition of carbon steel pipelines in oil and gas wells applications, 214 (2016) 347-356.
[28] A. Samakande, R. Chaghi, G. Derrien, C. Charnay, P.C. Hartmann, Aqueous behaviour of cationic surfactants containing a cleavable group, Journal of colloid and interface science 320(1) (2008) 315-320.
[29] R. Zana, Dimeric and oligomeric surfactants. Behavior at interfaces and in aqueous solution: a review, Advances in colloid and interface science 97(1-3) (2002) 205-253.
[30] C. Gamboa, A.F. Olea, Association of cationic surfactants to humic acid: Effect on the surface activity, Colloids and Surfaces A: Physicochemical and Engineering Aspects 278(1-3) (2006) 241-245.
[31] P. Patial, A. Shaheen, I.J.J.o.S. Ahmad, Detergents, Synthesis of ester based cationic pyridinium gemini surfactants and appraisal of their surface active properties, 16(1) (2013) 49-56.
[32] N. Negm, A. Al Sabagh, M. Migahed, H.A. Bary, H. El Din, Effectiveness of some diquaternary ammonium surfactants as corrosion inhibitors for carbon steel in 0.5 M HCl solution, Corrosion Science 52(6) (2010) 2122-2132.
[33] A.M. El-Shamy, M.M. Abdel Bar, Ionic liquid as water soluble and potential inhibitor for corrosion and microbial corrosion for iron artifacts, Egyptian Journal of Chemistry 64(4) (2021) 1867-1876.
[34] K. Ansari, M. Quraishi, A. Singh, Schiff's base of pyridyl substituted triazoles as new and effective corrosion inhibitors for mild steel in hydrochloric acid solution, Corrosion Science 79 (2014) 5-15.
[35] I. Abdelfattah, W. Abdelwahab, A. El-Shamy, Montmorillonitic clay as a Cost Effective, Eco Friendly and Sustainable Adsorbent for Physicochemical Treatment of Contaminated Water, Egyptian Journal of Chemistry 65(2) (2022) 687-694.
[36] G. Badr, The role of some thiosemicarbazide derivatives as corrosion inhibitors for C-steel in acidic media, Corrosion Science 51(11) (2009) 2529-2536.
[37] A. Dutta, S.K. Saha, U. Adhikari, P. Banerjee, D. Sukul, Effect of substitution on corrosion inhibition properties of 2-(substituted phenyl) benzimidazole derivatives on mild steel in 1 M HCl solution: a combined experimental and theoretical approach, Corrosion Science 123 (2017) 256-266.
[38] M. Behpour, S. Ghoreishi, N. Soltani, M. Salavati-Niasari, M. Hamadanian, A. Gandomi, Electrochemical and theoretical investigation on the corrosion inhibition of mild steel by thiosalicylaldehyde derivatives in hydrochloric acid solution, Corrosion Science 50(8) (2008) 2172-2181.
[39] S. Abd El Wanees, M.I. Alahmdi, M. Abd El Azzem, H.E. Ahmed, 4, 6-Dimethyl-2-oxo-1, 2-dihydropyridine-3-carboxylic acid as an inhibitor towards the corrosion of C-steel in acetic acid, Int. J. Electrochem. Sci 11(3448) (2016) e3466.
[40] S.A. Umoren, M.J. Banera, T. Alonso-Garcia, C.A. Gervasi, M.V. Mirífico, Inhibition of mild steel corrosion in HCl solution using chitosan, Cellulose 20(5) (2013) 2529-2545.
[41] S. Abd El Wanees, M.I. Alahmdi, S. Rashwan, M. Kamel, M. Abd Elsadek, Inhibitive Effect of cetyltriphenylphosphonium bromide on C-steel corrosion in HCl solution, Inter. J. Electrochem. Sci 11 (2016) 9265-9281.
[42] M. Bouklah, B. Hammouti, M. Lagrenee, F. Bentiss, Thermodynamic properties of 2, 5-bis (4-methoxyphenyl)-1, 3, 4-oxadiazole as a corrosion inhibitor for mild steel in normal sulfuric acid medium, Corrosion science 48(9) (2006) 2831-2842.
[43] A. Ehteram, H. Aisha, Thermodynamic study of metal corrosion and inhibitor adsorption processes in mild steel/1-methyl-4 [40 (-X)-styryl pyridinium iodides/hydrochloric acid systems, Mater Chem Phys 110 (2008) 145-154.
[44] M. Morad, A.K. El-Dean, 2, 2′-Dithiobis (3-cyano-4, 6-dimethylpyridine): A new class of acid corrosion inhibitors for mild steel, Corrosion science 48(11) (2006) 3398-3412.
[45] S. Abd El Wanees, N. ElBasiony, A. Al-Sabagh, M. Alsharif, S. Abd El Haleem, M.J.J.o.M.L. Migahed, Controlling of H2 gas production during Zn dissolution in HCl solutions, 248 (2017) 943-952.
[46] P. Mourya, S. Banerjee, M.J.C.S. Singh, Corrosion inhibition of mild steel in acidic solution by Tagetes erecta (Marigold flower) extract as a green inhibitor, 85 (2014) 352-363.
[47] R. Laamari, J. Benzakour, F. Berrekhis, A. Abouelfida, A. Derja, D.J.A.j.o.c. Villemin, Corrosion inhibition of carbon steel in hydrochloric acid 0.5 M by hexa methylene diamine tetramethyl-phosphonic acid, 4(3) (2011) 271-277.
[48] A.B. Radwan, M.H. Sliem, P.C. Okonkwo, M.F. Shibl, A.M.J.J.o.M.L. Abdullah, Corrosion inhibition of API X120 steel in a highly aggressive medium using stearamidopropyl dimethylamine, 236 (2017) 220-231.
[49] N. El Basiony, A. Elgendy, A.E. El-Tabey, A. Al-Sabagh, G.M. Abd El-Hafez, M. Abd El-raouf, M.J.J.o.M.L. Migahed, Synthesis, characterization, experimental and theoretical calculations (DFT and MC) of ethoxylated aminothiazole as inhibitor for X65 steel corrosion in highly aggressive acidic media, 297 (2020) 111940.
[50] H. Keleş, M. Keleş, I. Dehri, O.J.C. Serindağ, S.A. Physicochemical, E. Aspects, Adsorption and inhibitive properties of aminobiphenyl and its Schiff base on mild steel corrosion in 0.5 M HCl medium, 320(1-3) (2008) 138-145.
[51] A. Al-Sabagh, N. El Basiony, S. Sadeek, M.J.D. Migahed, Scale and corrosion inhibition performance of the newly synthesized anionic surfactant in desalination plants: Experimental, and theoretical investigations, 437 (2018) 45-58.

[52] J. Cruz, T. Pandiyan, E. Garcia-Ochoa, A new inhibitor for mild carbon steel: electrochemical and DFT studies, Journal of Electroanalytical Chemistry 583(1) (2005) 8-16.
[53] R. Fuchs-Godec, M.G. Pavlović, Synergistic effect between non-ionic surfactant and halide ions in the forms of inorganic or organic salts for the corrosion inhibition of stainless-steel X4Cr13 in sulphuric acid, Corrosion Science 58 (2012) 192-201.
[54] X. Li, S. Deng, H. Fu, Benzyltrimethylammonium iodide as a corrosion inhibitor for steel in phosphoric acid produced by dihydrate wet method process, Corrosion Science 53(2) (2011) 664-670.
[55] D.B.J.A.J.o.C. Matthews, The Stern-Geary and related methods for determining corrosion rates, 28(2) (1975) 243-251.
[56] A. Fekry, R.R.J.E.A. Mohamed, Acetyl thiourea chitosan as an eco-friendly inhibitor for mild steel in sulphuric acid medium, 55(6) (2010) 1933-1939.
[57] M.H. Sliem, M. Afifi, A. Bahgat Radwan, E.M. Fayyad, M.F. Shibl, F.E.-T. Heakal, A.M. Abdullah, AEO7 surfactant as an eco-friendly corrosion inhibitor for carbon steel in HCl solution, Scientific reports 9(1) (2019) 1-16.
[58] S.M. Shaban, A.A. Abd-Elaal, S.M.J.J.o.M.L. Tawfik, Gravimetric and electrochemical evaluation of three nonionic dithiol surfactants as corrosion inhibitors for mild steel in 1 M HCl solution, 216 (2016) 392-400.
[59] C.M. Goulart, A. Esteves-Souza, C.A. Martinez-Huitle, C.J.F. Rodrigues, M.A.M. Maciel, A.J.C.S. Echevarria, Experimental and theoretical evaluation of semicarbazones and thiosemicarbazones as organic corrosion inhibitors, 67 (2013) 281-291.
[60] F. Bentiss, F. Gassama, D. Barbry, L. Gengembre, H. Vezin, M. Lagrenée, M.J.A.S.S. Traisnel, Enhanced corrosion resistance of mild steel in molar hydrochloric acid solution by 1, 4-bis (2-pyridyl)-5H-pyridazino [4, 5-b] indole: electrochemical, theoretical and XPS studies, 252(8) (2006) 2684-2691.
[61] M. Hegazy, R. Samy, A. Labena, M.A. Wadaan, W.N.J.M.S. Hozzein, E. C, 4, 4′-(((1E, 5E)-pentane-1, 5-diylidene) bis (azanylylidene)) bis (1-dodecylpyridin-1-ium) bromide as a novel corrosion inhibitor in an acidic solution (part I), 110 (2020) 110673.
[62] M. Kamel, M. Hegazy, S. Rashwan, M.J.C.J.o.C.E. El Kotb, Innovative surfactant of Gemini-type for dissolution mitigation of steel in pickling HCl medium, 34 (2021) 125-133.
[63] M. Hegazy, H. Ahmed, A.J.C.S. El-Tabei, Investigation of the inhibitive effect of p-substituted 4-(N, N, N-dimethyldodecylammonium bromide) benzylidene-benzene-2-yl-amine on corrosion of carbon steel pipelines in acidic medium, 53(2) (2011) 671-678.
[64] M. Hegazy, M. Abdallah, H.J.C.S. Ahmed, Novel cationic gemini surfactants as corrosion inhibitors for carbon steel pipelines, 52(9) (2010) 2897-2904.
[65] S.M.J.J.o.M.L. Tawfik, Ionic liquids based gemini cationic surfactants as corrosion inhibitors for carbon steel in hydrochloric acid solution, 216 (2016) 624-635.
[66] A. Elgendy, A. Elkholy, N. El Basiony, M. Migahed, Monte Carlo simulation for the antiscaling performance of Gemini ionic liquids, Journal of Molecular Liquids 285 (2019) 408-415.
[67] N.E. Basiony, A. Elgendy, H. Nady, M. Migahed, E. Zaki, Adsorption characteristics and inhibition effect of two Schiff base compounds on corrosion of mild steel in 0.5 M HCl solution: experimental, DFT studies, and Monte Carlo simulation, RSC advances 9(19) (2019) 10473-10485.
[68] A. Al-Sabagh, N. El Basiony, S. Sadeek, M. Migahed, Scale and corrosion inhibition performance of the newly synthesized anionic surfactant in desalination plants: experimental, and theoretical investigations, Desalination 437 (2018) 45-58.
[69] G. Xia, X. Jiang, L. Zhou, Y. Liao, H. Wang, Q. Pu, J. Zhou, Synergic effect of methyl acrylate and N-cetylpyridinium bromide in N-cetyl-3-(2-methoxycarbonylvinyl) pyridinium bromide molecule for X70 steel protection, Corrosion Science 94 (2015) 224-236.
[70] M. Migahed, M. El-Rabiei, H. Nady, A. Elgendy, E. Zaki, M. Abdou, E. Noamy, Novel ionic liquid compound act as sweet corrosion inhibitors for X-65 carbon tubing steel: experimental and theoretical studies, Journal of Bio-and Tribo-Corrosion 3(3) (2017) 1-19.
[71] M. Masoud, M. Awad, M. Shaker, M. El-Tahawy, The role of structural chemistry in the inhibitive performance of some aminopyrimidines on the corrosion of steel, Corrosion Science 52(7) (2010) 2387-2396.
[72] T. Chakraborty, K. Gazi, D.C. Ghosh, Computation of the atomic radii through the conjoint action of the effective nuclear charge and the ionization energy, Molecular Physics 108(16) (2010) 2081-2092.
[73] M. ElBelghiti, Y. Karzazi, A. Dafali, B. Hammouti, F. Bentiss, I. Obot, I. Bahadur, E.-E. Ebenso, Experimental, quantum chemical and Monte Carlo simulation studies of 3, 5-disubstituted-4-amino-1, 2, 4-triazoles as corrosion inhibitors on mild steel in acidic medium, Journal of Molecular Liquids 218 (2016) 281-293.
[74] E.E. Ebenso, T. Arslan, F. Kandemirlı, I. Love, C.l. Öğretır, M. Saracoğlu, S.A. Umoren, Theoretical studies of some sulphonamides as corrosion inhibitors for mild steel in acidic medium, International Journal of Quantum Chemistry 110(14) (2010) 2614-2636.

[75] N. El Basiony, A. Elgendy, A.E. El-Tabey, A. Al-Sabagh, G.M. Abd El-Hafez, M. Abd El-raouf, M. Migahed, Synthesis, characterization, experimental and theoretical calculations (DFT and MC) of ethoxylated aminothiazole as inhibitor for X65 steel corrosion in highly aggressive acidic media, Journal of Molecular Liquids 297 (2020) 111940.
[76] I.B. Obot, E.E. Ebenso, M.M. Kabanda, Metronidazole as environmentally safe corrosion inhibitor for mild steel in 0.5 M HCl: experimental and theoretical investigation, Journal of Environmental Chemical Engineering 1(3) (2013) 431-439.
[77] E. Azzam, A.J.E.J.o.P. Abd El-Aal, Corrosion inhibition efficiency of synthesized poly 12-(3-amino phenoxy) dodecane-1-thiol surfactant assembled on silver nanoparticles, 22(2) (2013) 293-303.